3930
NACA TN 2544
TECH LIBRARY KAFB, NM
0065488

NATIONAL ADVISORY COMMITTEE FOR AERONAUTICS

TECHNICAL NOTE 2544

HYDRODYNAMIC LUBRICATION OF CYCLICALLY LOADED BEARINGS

By R. W. Dayton and E. M. Simons

Battelle Memorial Institute

Washington
November 1951

TECHNICAL LIBRARY
AFL 2811

TECH LIBRARY KAFB, NM

0065488

NATIONAL ADVISORY COMMITTEE FOR AERONAUTICS

TECHNICAL NOTE 2544

HYDRODYNAMIC LUBRICATION OF CYCLICALLY LOADED BEARINGS

By R. W. Dayton and E. M. Simons

SUMMARY

An experimental investigation of the hydrodynamic lubrication of cyclically loaded bearings was conducted in order to check the validity of the analytical studies of simple cases of cyclic loading and to determine the effect of the loading conditions on hydrodynamic lubrication when the load diagram is so complex that analytical treatment of the problem is difficult or impossible.

A precise test bearing was set up to which constant or varying unidirectional loads or constant rotating loads could be applied, singly or together, and the effect of the load diagram on hydrodynamic lubrication was measured from the attitude of the journal in the bearing.

Studies of film rupture due to tension in the oil film were conducted by running the bearing at no load and then photographing the spindle motions as an upward load was gradually applied. In accordance with expectations it was found that the higher the lubricant feed pressure, the higher the load that could be carried before film rupture occurred. The eccentricity ratio attained under a given load appeared to depend, within limits, upon whether rupture occurred and upon the extent of the rupture over the bearing surface.

When the test bearing was subjected to a rotating or sinusoidally alternating load, the shaft center moved in an orbit with eccentricity ratios which depended on the ratio of load speed N_p to spindle speed N_j. The mean frequency of rotation of the shaft center in its orbit was always equal to the frequency of loading. When N_p/N_j was 1/2, the eccentricity ratio was a maximum, but it did not reach unity as predicted by theory. This maximum eccentricity ratio could be lowered by increasing the speed, but it was not affected appreciably by changes in lubricant viscosity or external load.

INTRODUCTION

Although a number of theoretical studies (references 1 to 7) of the hydrodynamic lubrication of sleeve bearings subjected to rotating or varying loads have been published, very little experimental work has been reported to prove or disprove the conclusions of these studies. All theoretical treatments agree that dynamic loading of sleeve bearings produces behavior which cannot be predicted directly from the copious work which has been done using constant, unidirectional loads. Furthermore, the analyses indicate that there are certain speed and load conditions under which it is impossible for hydrodynamic lubrication to function properly.

Sleeve bearings in aircraft engines and accessories seldom operate with constant unidirectional loads. Certainly the load diagrams of most bearings in reciprocating internal-combustion engines are periodic and quite complex. Even in rotary aircraft engines, the reduction-gear bearings and other sleeve bearings may have appreciable nonsteady loads imposed by vibrations, by variations in power requirements, and by dynamic forces associated with maneuvering the aircraft.

Further mathematical investigations are hampered by the tremendous complexity of the problem when load diagrams with more than one component are considered.

Therefore, an experimental investigation was conducted to check the validity of the analytical studies of simple cases of cyclic loading and to determine the effect of the loading conditions on hydrodynamic lubrication when the load diagram is so complex that an analytical treatment of the problem is difficult or impossible.

The plan of this investigation was to set up a precise test bearing to which constant or varying unidirectional loads, or constant rotating loads, could be applied, singly or together, and to measure the effect of the load diagram on hydrodynamic lubrication, from the attitude of the journal in the bearing.

Initially, simple loading conditions were studied and then successively more complicated ones, as the simpler conditions were understood. The loading conditions which are of interest are:

(1) Unloaded

(2) Constant unidirectional loads

(3) Suddenly applied, constant loads

(4) Unidirectional loads, varying in magnitude

(5) Constant rotating loads

(6) Combinations of the above

This work was conducted at the Battelle Memorial Institute under the sponsorship and with the financial assistance of the National Advisory Committee for Aeronautics.

NOMENCLATURE

The symbols used in the discussions throughout the text are defined as follows:

r	radius of journal or bearing
w	axial width of bearing
c	radial clearance, or difference in radii of bearing and journal
e	distance between center of journal and center of bearing, called eccentricity
η	eccentricity ratio (e/c)
ρ	lubricant density
Δp	pressure drop from circumferential feed groove to end of bearing
μ	absolute viscosity of lubricant
φ	angle between direction of load and minimum film-thickness end of line of centers, measured in direction of rotation
N_j	average rotational frequency of journal in revolutions per unit time
N_p	average frequency of rotation or oscillation of load, in revolutions or cycles per unit time
N_e	mean frequency of rotation of journal center in its orbit, revolutions per unit time

M mass of rotor whirling with eccentricity e

F external load applied to bearing

P load per unit projected area of bearing $(F/2rw)$

S Sommerfeld variable or Sommerfeld number $\left(\left(\frac{r}{c}\right)^2 \frac{\mu N_j}{P}\right)$

Definitions:

Line of centers: Line determined by center of journal and center of bearing

Clearance circle: Locus of journal center for $\eta = 1$; this is a circle whose radius is c

Indicated clearance circle: Clearance circle as it appears on micrometer oscilloscope screen

EXPERIMENTAL WORK

Apparatus

A photograph of the testing machine designed and constructed for this study is presented as figure 1. A complete description of the machine and the associated measuring apparatus is given in appendix A.

Briefly, with this machine it is possible to apply to a test bearing any steady load from 0 to 500 pounds, any suddenly applied or unidirectionally varying load of the same magnitude, or a constant rotating load of the same magnitude. The frequency of journal rotation and the frequency of the loading cycle can be varied over a considerable range. An electric micrometer (reference 8) is used to reveal the condition of hydrodynamic lubrication by indicating, at any instant, the position of the center of the journal in the bearing. The instrument draws a trace on an oscilloscope screen of the magnified movement of the shaft center and follows either very slow or very rapid motions.

During the first phase of this study, several faults were discovered in the testing machine which rendered accurate interpretation of results impossible. Changes were therefore made to eliminate these defects and these changes are discussed in appendix B.

Three lubricants were used in the experimental work: SAE 10 motor oil, kerosene, and straw paraffin oil, all desulfurized. Their specific gravities and viscosities are listed in the following table and temperature-viscosity curves are shown in figure 2.

PROPERTIES OF LUBRICANTS

Lubricant	Temperature (°F)	Specific gravity	Kinematic viscosity (centistokes)
SAE 10 oil	100	0.861	38.0
	130	.851	21.4
	176	.831	10.1
	210	.824	5.8
Kerosene	66	.8062	2.16
	100	.7986	1.59
	130	.7789	1.30
Straw parafin oil	78	.8753	21.26
	100	.8706	14.33
	130	.8630	8.40

Journal Whirl

Reduction of free whirl by pivoted-pad main bearing.- Early in this study it was found that, with SAE 10 oil, the combination of oil pressures in the two circumferential grooves of the test bearing determined whether the spindle center assumed some equilibrium position or moved indefinitely in a circular orbit under no load. When the pressure in the right groove was high, the shaft center moved in an orbit, whereas, when the left-groove pressure was high, the shaft center was stationary.

Recently, the sleeve-type main bearing was replaced by a pivoted-pad bearing, a type which does not whirl. The behavior of the test bearing in whirl is now completely different. There appear to be no circumstances which produce sustained whirling of the shaft. Apparently, either the original sleeve-type bearing had produced an excitation for whirl, or, more probably, the present type of bearing has a slight damping action on the whirling motion.

Since whirling would not continue indefinitely with the present arrangement of the apparatus, the only free-whirl studies which could be made were those of transient whirling during starting. The observations are reported in more detail in the section on starting transients, but a few general comments will be made here.

Frequency of no-load whirling.- Swift (reference 3) has demonstrated mathematically that in a bearing under no load, whirling occurs in a circular orbit at any eccentricity whatsoever, with an angular velocity exactly half of the journal speed. Using the method of measuring whirl frequency described in appendix C, it was found that the natural whirl during no-load starting occurred at slightly less than one-half the shaft speed, as seen in the following table.

FREQUENCY OF NO-LOAD SHAFT WHIRL, WITH SAE 10 OIL

Spindle speed, N_j (rpm)	N_e/N_j (Flood lubrication)	N_e/N_j (50 lb/sq in. gage feed pressure)
154	0.4980	0.4971
380	.4968	------

Hagg (reference 9) states that one-half the rotational frequency is the upper limit of whirling frequency for an unloaded ideal bearing, but that "in reality, this upper limit is reduced because of fluid friction and bearing leakage." If this is true, it would explain why the values of N_e/N_j in the table were less than 0.500. However, the authors fail to see how fluid friction and side leakage alter the simple theory which demonstrates that an unloaded journal should whirl at one-half the shaft speed.

It is agreed that any whirling which occurs in a steadily loaded bearing will take place at less than one-half the shaft speed, the actual frequency ratio decreasing with increasing load (reference 3). However, the theoretical steady load required to produce a speed ratio of 0.4980 was found to be appreciable, and no source of such a load could be found.

Factors influencing shaft whirl.- Swift's work would indicate that, in general, the journal center would not be stationary under no load, or even under a constant load. On the contrary, the experiments have shown that the ultimate equilibrium position of the journal center was always a stationary spot, in the absence of external periodic excitation. Failure of the theory to consider the damping forces which prevent the journal center from moving continually in an orbit constitutes the most likely explanation for the observed departures from theoretical predictions. Experimentally, it was found that the most rapid damping of journal whirl was obtained with high steady loads, high shaft speeds, high lubricant feed pressures, or low-viscosity lubricants.

A simplified theoretical study was made of the forces exerted on the shaft by the centrifugal action accompanying whirling and by the circumferential pressure gradient in the lubricant caused by Bernoulli forces. In the present case, with circumferential oil grooves, Bernoulli forces arise because of the axial oil flow caused by a uniform pressure in the oil grooves. Where the separation of the shaft and bearing is greatest, the lubricant velocity will be greatest and the static pressure will be least. Hence, the resultant oil-pressure force tends to push the shaft toward the center of the clearance space. There is also a centrifugal force on an eccentrically rotating shaft, which acts in the opposite direction, so as to increase the eccentricity.

If no damping were present, the diameter of the no-load circular orbit would be determined by the eccentricity ratio at which the centralizing pressure force was numerically equal to the decentralizing centrifugal force. A quantitative discussion of these forces in the test bearing is presented in appendix D. With the present arrangement of the apparatus, it appears that there is sufficient damping to prevent continuous whirling under any conditions which have been examined. This is so because the low rotative speeds used in the tests produced centrifugal forces which were small and easily overcome by the inherent damping.

Importance of whirl.- In certain machines, such as high-speed turbine compressors, where the centrifugal forces are large, sustained whirling of sleeve-type bearings would be expected, at an eccentricity ratio close to 1. The simplified analysis of an aircraft-turbine-compressor sleeve bearing, presented in appendix D, demonstrates the seriousness of this effect.

Whirling of sleeve-type bearings could be troublesome in many other applications. For example, in machine-tool spindles, shaft whirl causes inaccuracies in machining and undesirable surface roughness. Whirling in sleeve-type propeller-shaft bearings, such as aircraft and marine shaft bearings, could contribute to fatigue-induced failures.

Of the whirl-damping influences mentioned previously, namely, high steady loads, high shaft speeds, high lubricant feed pressures, and low-viscosity lubricants, experiments indicate that the reduction of lubricant viscosity has a greater effect than the others. This observation suggests that troublesome whirling in certain machines might be minimized by a change to a lower-viscosity lubricant.

Studies of Unidirectional Steady Loads

Oil-film tension.- In a flooded full journal bearing, the theoretical pressure distribution over the semicylinder on one side of the line of centers is the exact negative reflection of that on the semicylinder on the other side of the line of centers. This condition implies that the integrated pressure-area product in the film can have no component along the line of centers, so that the displacement of the journal in the bearing must be normal to the direction of load application. It also indicates that when a flooded full journal bearing is operating with an unbroken oil film, half the external load is supported by hydrodynamic pressures above atmospheric on the loaded side, and the other half, by equal pressures below atmospheric on the unloaded side. For example, if the external load is 10 pounds per square inch, the average negative pressure on the unloaded side will be 5 pounds per square inch, and the peak negative pressure may be three times the average, or 15 pounds per square inch.

If this peak negative pressure exceeded 1 atmosphere, the oil film would rupture in the region of theoretical pressures below absolute zero, unless the film were capable of carrying a tensile load. In the latter case, the rupture would occur when the negative pressures exceeded the tensile strength of the oil film. Any such break in the film will require that the journal move in the direction of loading and result in higher eccentricities than those predicted by hydrodynamic theory. This implies that a flooded journal bearing would operate with a continuous film only when the external loads were less than about 10 pounds per square inch, assuming that the peak pressure developed in the oil film is about three times the average. However, the application of feed pressures in the circumferential oil grooves of the test bearing makes it possible to support higher loads without film rupture, because the feed pressure helps to prevent a tensile stress in the oil film.

Studies of the behavior of a unidirectionally loaded bearing were conducted by running the bearing at no load and photographing the spindle motions as an upward load was applied gradually enough to maintain equilibrium at all times. Some pictures taken in this way are presented in figure 3. In figure 3(a), the shaft moved horizontally (normal to the direction of loading), in accordance with the theory, until the external

load reached about 20 pounds per square inch. At this point, the negative pressures became too great, the oil film ruptured, and the shaft moved upward, in the direction of the load. As the feed pressures were increased (figs. 3(b) and 3(c)), the rupture occurred at higher and higher loads, until, at a feed pressure of about 15 pounds per square inch gage, the film remained apparently intact under the total load of 50 pounds per square inch (cf. fig. 3(d)), and no upward motion of the shaft took place. The rupture occurs suddenly in some cases, as evidenced by a sharp break from horizontal to upward motion, such as in figures 3(a) and 3(c).

Rough calculations of the magnitude of the negative film pressures appear to indicate that the oil film is withstanding a small tension, from a few to 50 pounds per square inch. It is known that liquids can withstand a tensile force under some circumstances, and conditions in a bearing appear to be favorable.

Effect of film rupture on eccentricity.- Qualitative studies of film rupture were made with a Lucite bearing on a steel shaft, observing the film conditions with ultraviolet light. The lubricant was introduced at a point source in the unloaded region of the bearing. It was found that film rupture started in localized areas on both sides of the oil hole, the evacuated areas extending, at times, for some distance circumferentially but seldom reaching axially to the outside edges of the bearing. These observations led to the belief that film rupture, originating in a highly localized region of peak negative pressure and extending over only a small fraction of the axial bearing length, results in a redistribution of pressures on the unloaded side of the journal. Only when the load becomes high enough to rupture the film over a sizable fraction of the bearing area does the shaft move in the direction of the load, the amount of motion and, hence, the eccentricity depending upon the extent of the rupture. This hypothesis could partially explain the apparent high tensile strengths of oil films mentioned.

This concept of the dependence of eccentricity ratio upon the extent of film rupture is verified by the experimental results shown in figure 4, which is a plot of eccentricity as a function of Sommerfeld number. The lowest circled points agree, within experimental accuracy, with the theoretical curve from Muskat and Morgan (reference 10), based on a continuous oil film. A second curve, drawn through the points showing the greatest departure from the theoretical curve, represents the cases where the oil feed pressure was low (flood lubrication) and film rupture had occurred to the greatest extent. Between these two curves are eccentricities which result from various degrees of film rupture, the points lying closest to the lower curve representing highly localized areas of rupture, and those lying near the upper curve representing rupture over more extensive areas. This range of eccentricity ratios

was produced, at a given Sommerfeld number, by varying the oil feed pressure in the circumferential grooves, as illustrated in figure 3.

Practically all theoretical treatments of journal bearings assume continuity of the oil film around the bearing arc. Figure 4 demonstrates that these theories cannot be used to predict experimental results unless the experiments are conducted with high enough lubricant feed pressures or low enough external loads to preclude rupture at any point in the oil film.

Sudden-Load Tests

Means have been provided in the testing machine for applying a sudden, preset steady load to the bearing, while it is running under no load. It was noted that, after the transient motions, which occurred immediately after the load was suddenly applied, were completed, the journal center assumed the position it would normally have occupied under the same steady load. In other words, the ultimate equilibrium position of the shaft center was not affected by the fact that the load application had been sudden. However, the path which the shaft center followed in going from the unloaded to the loaded equilibrium position was definitely influenced by the suddenness of the load.

When the load was applied gradually, as in figure 3, the shaft moved at right angles to the load line, in accordance with the theory governing steady loads. However, when the load was suddenly applied, it may be seen from figure 5 that the shaft motion started out in the direction of the load. If, as discussed in the section on film rupture, the external load and feed pressure were such that the oil film could not rupture permanently, then the journal center moved in an arc to an equilibrium position in which the line of centers was normal to the load line (figs. 5(a) and 5(c)). On the other hand, if the feed pressure were too low to prevent film rupture under the applied load, the equilibrium position of the shaft center was displaced upward, in the direction of loading, as in figure 5(b).

When the lubricant was kerosene, the shaft moved very quickly to the new equilibrium position immediately after the load was applied (figs. 5(a) and 5(b)). With straw paraffin oil, the shaft approached the loaded equilibrium position in a tight spiral (fig. 5(c)) before finally settling down. This behavior is in accord with the high whirl-damping influence attributed to low-viscosity lubricants, as discussed in the section on starting and stopping.

Starting and Stopping

Starting under no load.- When the shaft was started from rest under no load, it moved in a spiral toward the center of the bearing with a mean angular velocity in its orbit of just under one-half the shaft speed, as previously discussed. Regardless of the combination of variables tried, the spiral always ended in a steady spot at the center of the bearing. However, the conditions of the particular test determined how quickly this equilibrium position was reached.

High shaft speeds, high lubricant feed pressures, and low-viscosity lubricants all favored more rapid steadying of the shaft. The damping effect of higher lubricant pressures on whirling can be seen by comparing parts (a) and (b) of figure 6; the damping effect of high speeds is strikingly shown by comparison of figure 6(b) with figure 6(c), while the steadying influence of low viscosity is evident from the fact that it always took much longer to reach equilibrium when higher-viscosity lubricants were used at the same speed and lubricant feed pressure.

Starting under steady load.- Figure 7 shows the motion of the spindle center when started from rest under an upward load of 50 pounds per square inch. It is commonly thought that, upon starting from rest, the shaft crawls along the bearing wall in a direction opposite to that shown, until solid friction is reduced sufficiently by the formation of an oil film for hydrodynamic forces to take over. This effect is not observable in figure 7, indicating that the oil film was generated much more rapidly than is usually assumed and that the crawling motion, if present at all, was too small to be detected in the photograph.

Starting at the top of the clearance space, the shaft moved down and to the left as it came up to speed and its load-carrying capacity increased. It then moved toward the center of the clearance circle, finally stabilizing at an eccentricity ratio of 0.27, which agrees with the theoretical predictions of Muskat and Morgan (reference 10).

The absence of full spiralling motions like those obtained with no-load starting is apparent. Indeed, it has been found that free whirling of the journal is strongly damped by the application of an external load.

Stopping transients.- When the shaft was stopped under 50-pound-per-square-inch upward load, its center retraced exactly the path of figure 7 moving to the left and then upward as the rotational motion slowed down and the load-carrying capacity of the oil film decreased.

Constant Load Rotating at Constant Speed

Importance of rotating loads.- Bearings subjected to rotating loads are encountered in many common machines. Slight unbalance in high-speed shafts may subject the bearings to relatively large centrifugal loads. The reduction-gear bearings of rotary aircraft engines may have appreciable cyclic loads imposed by vibrations resulting from gusts and by gyroscopic forces associated with maneuvering the aircraft. Once a rotor starts to whirl in its bearings, the centrifugal forces resulting from the eccentricity tend to maintain or even increase the amplitude of whirl. Consequently, a knowledge of the effect of rotating loads on hydrodynamic lubrication would be very useful in bearing design. Since the hydrodynamic forces developed in a sleeve-bearing oil film depend not only upon the rotation of the journal about its own center but also upon the motion of the whole shaft in the clearance space, it is apparent that any orbital motion of the journal center imposed by a constant rotating load will, in general, produce an eccentricity different from that given by the same load applied unidirectionally.

Shaft rotating.- Figure 8 shows the eccentricities resulting from the application of a 7.8-pound-per-square-inch load rotating at various frequencies. The ratio $N_p/N_j = 0$ represents a constant unidirectional load, and the value of η here agrees with Muskat's prediction (reference 10) for a flooded full journal bearing under these conditions. As N_p/N_j is increased, η_{max} increases also, peaking sharply at $N_p/N_j = 0.5$. Further increase in N_p/N_j is accompanied by a drop in η_{max}, which has the same value at $N_p/N_j = 1.0$ as at $N_p/N_j = 0$. This agrees with the findings of Burwell (reference 7) and Underwood (reference 11), namely, that a bearing subjected to a constant rotating load applied at the frequency of shaft rotation has a load capacity numerically the same as if the load were stationary. Frequency ratios greater than 1.0 yield eccentricities lower than those obtained by constant unidirectional loading.

The equations relating the variables in the case of a constant load rotating at constant speed are found (references 7 and 2) to be

$$\frac{\eta}{\left(2 + \eta^2\right)\sqrt{1 - \eta^2}}\left(1 - 2\frac{N_p}{N_j} - 2\frac{1}{2\pi N_j}\frac{d\varphi}{dt}\right) = \frac{1}{12\pi^2 S}\sin\varphi \tag{1}$$

$$\frac{1}{\left(1 - \eta^2\right)^{3/2}}\frac{1}{2\pi N_j}\frac{d\eta}{dt} = \frac{1}{12\pi^2 S}\cos\varphi \tag{2}$$

These are based on the following assumptions:

(1) No end leakage

(2) Continuous oil film around the bearing

(3) No local changes in viscosity

(4) The oil has no inertia

(5) Oil pressure is constant along a radius

If no motion of the journal center relative to the direction of the load is assumed $\left(\frac{d\eta}{dt} = \frac{d\varphi}{dt} = 0\right)$, the equations reduce to

$$\frac{\eta}{\left(2 + \eta^2\right)\sqrt{1 - \eta^2}}\left(1 - 2\frac{N_p}{N_j}\right) = \pm \frac{1}{12\pi^2 S} \tag{3}$$

$$\varphi = \pm \frac{\pi}{2} \tag{4}$$

Equation (4) states that the angular position of the line of centers is always at right angles to the direction of the load. To check this experimentally, a contactor was fastened to the rotating load device to produce a brightening of the spot on the oscilloscope screen every time the load was in some known direction. It was found that, while the period of rotation of the line of centers was the same as the period of load application, the phase angle φ between the line of centers and the load line was not ordinarily 90°. Furthermore, the angular velocity of the line of centers was generally not constant; hence, the phase angle varied during each revolution. For example, figure 9 shows the phase angles for the indicated load directions, with $N_p/N_j = 1/6$, in the flooded bearing. The fluctuations in angular velocity of the journal center were quite noticeable, there being a distinct pause when the load was at about 190° and a less-pronounced pause at about 75°. When the oil feed pressure was increased, the character of the orbit changed noticeably, the "pauses" becoming small loops, with much greater fluctuation in eccentricity ratio during each cycle. Though the phase angles were considerably closer to 90° in the pressure-fed bearing, the

variation in angular velocity of the shaft center was still apparent. The differences in performance between the flooded bearing and the pressurized one are related to film-rupture phenomena discussed previously.

Now, since equations (3) and (4) assume both η and φ constant with time, the fact that $d\varphi/dt$ was found experimentally to have positive negative values during each cycle and that η was not constant might account for the departures of the phase angle from the predicted 90° and invalidates equations (3) and (4). When $N_p/N_j = 1/2$, the fluctuations in η and φ were found to be quite small, the line of centers lagging behind the load line by about 30° during the entire cycle. This observation was made with $N_j = 150$ rpm, a 12.5-pound-per-square-inch load rotating at 75 rpm, with SAE 10 oil in the bearing. Variation in feed pressure had no noticeable effect on phase angle, eccentricity, or character of the orbit.

One method of checking the validity of differential equations (1) and (2) would be to perform a numerical integration with experimentally determined boundary values of η and φ and see whether the resulting journal-center motion corresponds to that observed.

When the load is rotating at one-half the shaft speed, equation (3) indicates that the bearing will not carry any load with an eccentricity ratio other than unity. In the experiments, it was found that the peak eccentricity ratio was less than unity, decreasing slowly with decreasing load and decreasing rapidly with increasing speed. These effects are apparent in figure 10.

One possible explanation for the presence of an oil film, in violation of the theoretical predictions when $N_p/N_j = 0.5$, lies in the discarding of higher-order terms in the development of the theory (reference 2). However, when this was investigated by substituting test conditions into the discarded terms, it was found that these terms were truly negligible, causing theoretical changes in eccentricity which were considerably smaller than the accuracy of experimental measurements.

Another likely source of the discrepancy was the possibility of a dynamic stiffening effect, in the pivoted-pad main bearing, which might prevent the journal from attaining the maximum eccentricity in the test bearing. The stiffening would have to stem from dynamic forces, since it was possible to maintain contact between journal and bearing while rotating the load a full revolution slowly by hand. To ascertain the role of main-bearing hydrodynamic forces in stiffening, test-bearing motions were studied first with SAE 10 oil in the main bearing and then with kerosene in the main bearing, while maintaining constant conditions at the test bearing. The tests showed that the viscosity of the lubricant

in the main bearing had no effect on the eccentricity in the test bearing, indicating strongly that main-bearing stiffness did not limit journal motions in the test bearing.

A third explanation proposed for the nonunit eccentricity ratios obtained with $N_p/N_j = 0.5$ was that gyroscopic forces might oppose the hydrodynamic effects. However, simple computations showed that, because of the low journal speeds used in tests, gyroscopic forces were much too small to have any noticeable effect on eccentricity.

It is true that the eccentricity rises to a sharp peak when $N_p/N_j = 0.5$ (fig. 8) and that it is best to avoid such conditions in practice whenever possible. It would be desirable to ascertain what physical conditions prevent the eccentricity ratio from reaching the theoretical value of unity when $N_p/N_j = 0.5$. A knowledge of the factors which are favorable to the maintenance of an oil film under these conditions could provide valuable aid in the design of sleeve bearings for applications where cyclic load components at or near one-half the frequency of shaft rotation are unavoidable. In an effort to obtain some clue from the appearance of the test bearing, the shaft was removed and the bearing studied. Burnish marks near both ends of the bearing gave strong indication that the shaft and bearing axes were not parallel. A very careful check with sensitive dial indicators revealed the fact that the axes diverged by 0.0006 inch in the 3-inch housing length. This misalinement was reduced to 0.00015 inch by straining the housing supports with short lengths of arc weld, which contracted the parent metal, causing the housings to move in the proper directions.

EFFECT OF BEARING MISALINEMENT ON ECCENTRICITY, WITH

ROTATING LOAD AT ONE-HALF SHAFT SPEED

[Rotating load, 12.5 lb/sq in. at one-half shaft speed;
SAE 10 oil, flood lubrication]

Shaft speed (rpm)	Eccentricity ratios	
	0.0006-in. misalinement	0.00015-in. misalinement
150	0.72	0.83
300	.61	.66

The above table shows that this improvement in alinement resulted in a closer approach to the theoretical eccentricity ratio of unity when $N_p/N_j = 1/2$, indicating that misalinement is probably a contributing factor in the discrepancy between theory and experiments.

That misalinement might prevent a zero oil-film thickness when $N_p/N_j = 1/2$ can be seen from the qualitative discussion which follows. Assuming that center A (see following sketch) whirls in a circular orbit,

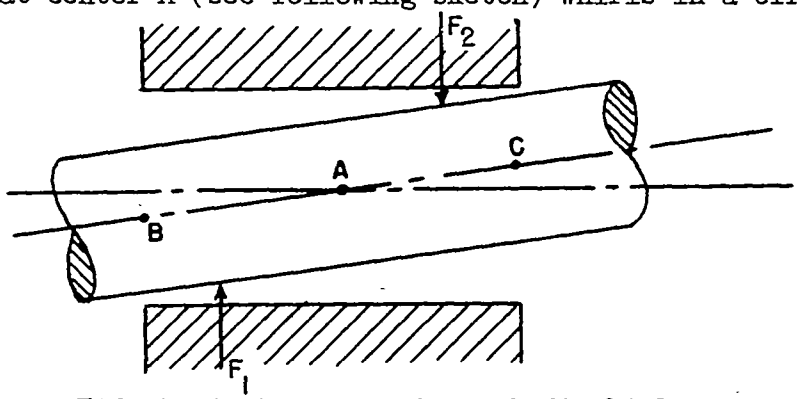

Effect of misalinement on shaft whirl.

B and C are forced to rotate in circular orbits also (since one end of the shaft is essentially fixed), but the centers of the latter orbits will be displaced, respectively, below and above the center line of the bearing. This nonconcentric whirling of the shaft at every section except A will produce varying hydrodynamic forces F_1 and F_2, equivalent to external loads superimposed on the applied roating load. As will be discussed in a later section of this report, such combined loads may reduce the eccentricity below that which would result from the rotating load alone, applied at one-half the shaft speed. Furthermore, an increase in shaft speed would increase the hydrodynamic forces F_1 and F_2 and further reduce the eccentricity. This agrees with the experimental results in figure 10 and in the preceding table.

Additional theoretical and experimental study along these lines is needed before more definite conclusions can be drawn. However, the results suggest the possibility of controlling shaft whirling by introducing controlled misalinement between the bearing and shaft axes.

Shaft stationary.- It was thought that the indicated clearance circle could be obtained rather easily by applying a rotating load to the stationary shaft and photographing the orbit on the oscilloscope screen after all the oil had been squeezed out of the bearing. Actually, it was found impossible to squeeze all the oil out of the clearance space in any reasonable time after oil shut-off.

Typical results of these experiments are shown in figure 11. The eccentricities were small as long as lubricant was being fed to the test bearing, increasing very rapidly in the first minute after oil shut-off, and increasing very slowly from then on. The eccentricities were very sensitive to frequency of load rotation, approaching zero with increasing speed, even after the oil had been shut off for a long time.

An unsuccessful attempt was made to remove all lubricant from the test bearing by thorough flushing with petroleum ether and drying with compressed air. Even after this treatment, it was not possible to obtain an eccentricity ratio of unity by applying a 200-pound load, rotating at 97 rpm, to the stationary shaft. The maximum eccentricity ratio reached in this test was 0.82, 1/2 minute after starting the load rotation. It was concluded, therefore, that this technique was unsatisfactory for obtaining the indicated clearance circle.

Information was obtained on the phase angle between the load direction and the line of centers. It was found, in the above tests, that the line of centers lagged behind the load line by an angle which varied from 0° to 90°, depending on whether the speed was low or high, respectively. The only way in which the zero phase angle could be obtained was by rotating the load very slowly by hand, and in this case the shaft center traced out the true clearance circle. However, when the load was driven at any appreciable speed, the eccentricity ratio was always less than unity, and the phase angle was always greater than 0, in spite of the fact that no oil was being supplied to the bearing.

These effects are not understood as yet. Further studies of the consequences of misalinement, local heating, or inertia forces might throw some light on the subject.

Sinusoidal Alternating Load in Vertical Direction

Burwell (reference 7) has extended the hydrodynamic theory of lubrication to the general case of a periodic load and has applied his findings to the solution of the problem of a sinusoidal reciprocating load with a journal rotating at constant speed. Since no analytical solution to his differential equations could be found, he carried out the solution by a step-by-step numerical integration, using a trial-and-error process to obtain closed-path solutions in one cycle of load application. His computations for the case of $N_p/N_j = 1/2$ lead to the same conclusion arrived at by Dick (reference 6), namely, that the oil film will not support a sinusoidal load applied at this frequency.

Just as in the case of rotating loads, the theory was not substantiated by experiments with sinusoidal loads applied at one-half the

frequency of shaft rotation, as may be readily seen from figures 12, 13, and 14. An oil film definitely existed in all experiments, and this film increased in thickness as the Sommerfeld variable was increased.

Burwell's calculations produced orbits which resemble ellipses for sinusoidal alternating loads. He found that the long axis was in the direction of loading when N_p/N_j was greater than 1/2 and that the long axis was perpendicular to the load line when N_p/N_j was less than 1/2. At $N_p/N_j = 1/2$, his orbit was the clearance circle. These shapes agree rather well, in general, with experimental findings, as may be seen from the examples in figure 15. Furthermore, as Burwell pointed out, the paths become more complicated for values of N_p/N_j less than about 1/4. His orbit for $N_p/N_j = 1/4$ did not exhibit the extra loop shown in figure 16(a), but this discrepancy can perhaps be attributed to the wide divergence between his value of S_{min} (0.01) and that used in the experiment (2.38). Figure 16(b) shows an interesting symmetric double-loop pattern obtained with $N_p/N_j = 1/6$. The complicated gyrations of the shaft center before finally settling down to an equilibrium orbit are illustrated by figure 16(c), which was photographed $1\frac{1}{2}$ minutes after the shaft had been started from rest. It took an additional $1\frac{1}{2}$ minutes to reach an equilibrium orbit similar in shape to figure 15(a). Most of the frequency ratios tested produced equilibrium orbits which closed in one cycle of load application. The exception to this was $N_p/N_j = 0.7$, in which case the path was an oscillating spiral between a larger and a smaller orbit. The time required to reach equilibrium, the complex transient patterns traced by the shaft center before equilibrium was reached, and the character of the ultimate equilibrium orbit indicate that certain N_p/N_j ratios produce equilibrium orbits which close in one loading cycle only as a result of external damping conditions, or the fact that particular initial conditions existed. The behavior is analogous to the forced vibrations of a resonant system, in which the equations of motion contain terms dependent upon initial conditions and upon the resonant frequency. These terms can be neglected only after damping has eliminated the effect of initial conditions. There is a great deal of room for further work in correlating the theory with experiments.

Since the orbits were not circulr, except when $N_p/N_j = 1/2$, it was possible to measure a maximum and a minimum eccentricity. Plots of these values for two different values of S_{min} are shown in figure 12.

When the load was applied at a very low frequency $\left(N_p/N_j = 0\right)$, the eccentricity varied from 0, when the load was 0, to a maximum which corresponded to the peak load applied continuously. As N_p/N_j was increased, both η_{max} and η_{min} increased, η_{min} increasing faster than η_{max} until N_p/N_j reached 0.5, at which point $\eta_{min} = \eta_{max}$ and the orbit was circular. Further increase in N_p/N_j resulted in a rapid drop in eccentricity, with η_{max} falling considerably below that for the constant unidirectional load, at values of N_p/N_j above about 0.65. These observations correspond generally to the relative load-capacity curves presented by Burwell (reference 7) and Underwood (reference 11).

In figure 13, the very small influence of magnitude of load on eccentricity for sinusoidal loading at $N_p/N_j = 1/2$ is demonstrated. Above loads of about 6 pounds per square inch, the eccentricity increased only slightly for large increases in load; while, as may be seen in both figures 12 and 13, the eccentricity dropped rapidly as the speed was increased. Figure 14 shows that, for a given Sommerfeld number, low viscosities favored thick lubricant films. Figures 13 and 14 are convincing evidence that, as the theory predicts, hydrodynamic lubrication is inoperative in bearings subjected to sinusoidal alternating loads at and near one-half the frequency of shaft rotation. The Sommerfeld variable, which is a parameter of true hydrodynamic lubrication, is not important under these conditions. Varying the viscosity or load, in a given test, seems to have little effect on the eccentricity when $N_p/N_j = 1/2$, while changing the speed has a pronounced effect. The origin of load-supporting pressures in the lubricant film is not known.

Combined Rotating and Alternating Loads

A series of tests was run with a combination of rotating and alternating loads. The rotating load was 12.5 pounds per square inch applied at the frequency of shaft rotation to simulate centrifugal loading. The sinusoidal alternating load was from -12.5 to 12.5 pounds per square inch, applied at one-half the spindle speed to represent, for example, gas-pressure loading in a four-stroke-cycle engine crankshaft bearing.

The results are presented in figure 17, parts (a) and (b) being photographed under the same conditions except for a 90° phase change in the relationship between the rotating and alternating loads. It is apparent that the eccentricities are considerably greater than those which would result from the same loads applied steadily, and it is also obvious that the phase relationship between the centrifugal and gas-pressure loads has some slight effect on the eccentricity. However, the

observation of greatest significance is that the alternating load alone (fig. 17(c)) applied at half the shaft frequency produced an eccentricity ratio which was greater than that resulting from the combined loads, even though the combined load peaks were as much as twice those of the alternating load alone. Furthermore, figure 18 shows that the higher the superimposed rotating load, the thicker the operating oil film. This phenomenon helps to explain why four-stroke-cycle engine crankshaft bearings can operate with complete film lubrication, in spite of the gas-pressure loading at the critical frequency of one-half the shaft speed; for the inertia and centrifugal load components tend to reduce the eccentricity in the same manner as was found in the experiments.

In view of the foregoing discussion, it is entirely possible that troublesome whirling in sleeve bearings can be reduced to a safe operating level by the addition of a rotating load at the frequency of shaft rotation – for example, by purposely introducing some unbalance in the rotating members and taking care of the resulting vibration by vibration-isolation mounts.

DISCUSSION AND RESULTS

The experimental investigation of the hydrodynamic lubrication of cyclically loaded bearings was carried out in order to check the validity of analytical studies of simple cases of cyclic loading and to determine the effect of the loading conditions on hydrodynamic lubrication when the load diagram is so complex that analytical treatment of the problem is difficult or impossible.

The testing machine built for this study incorporated an accurately lapped spindle in precision-bored bearings, a lubricant supply system, and means for applying steady, alternating, and rotating loads to the test bearing according to some selected diagram. The variable chosen as a sensitive indicator of the effectiveness of hydrodynamic lubrication, the position of the center of the journal in the clearance space, was measured with a radio-frequency micrometer of high sensitivity.

A number of alterations were made to the apparatus during the investigation. Replacement of the sleeve-type main bearing by a stiff pivoted-pad bearing accomplished its purpose of maintaining one end of the shaft essentially fixed while measurements were being made of spindle motions at the other end. The radio-frequency micrometer was rebuilt and made more stable and linear. A new silver-plated test bearing was installed and precision-bored with a taper, such as to keep the shaft surface approximately parallel to the test bearing surface along the line of closest approach. By providing more positive clamping, the

linearity of calibration of the micrometer probe cantilevers was improved considerably.

Conclusions drawn from starting, stopping, and sudden-load tests were essentially the same as those found before the changes were made, with the exception that it was not possible to produce sustained orbital motion of the journal. Also, it was found that the amount of whirling during starting was substantially reduced. Apparently, either the original sleeve-type bearing provided excitation for whirling or the pivoted-pad bearing has a damping action on whirling. Factors tending to damp journal whirl were found to be high nonperiodic loads, high shaft speeds, high lubricant feed pressures, and low-viscosity lubricants.

Studies of film rupture due to tension in the oil film were conducted by running the bearing at no load, then photographing the spindle motions as an upward load was gradually applied. Theoretically, as long as the negative pressures are sustained, the oil film remains intact and the shaft moves at right angles to the direction of load application. When the load is sufficiently high to overcome the influence of feed pressures in the circumferential grooves and to cause rupture of the oil film, the shaft moves in the direction of the load. The experiments showed that, in accordance with expectations, the higher the lubricant feed pressure, the higher the load that could be carried before film rupture occurred. The eccentricity ratio attained under a given load appeared to depend, within limits, upon whether rupture occurred and upon the extent of the rupture over the bearing surface. There was some indication that the oil film has an unexpectedly high tensile strength, although sufficient quantitative data were not obtained to make this observation conclusive.

When the test bearing was subjected to a rotating or sinusoidally alternating load, the shaft center moved in an orbit with eccentricity ratios which depended on the ratio of load speed N_p to spindle speed N_j. The mean frequency of rotation of the shaft center in its orbit was always equal to the frequency of loading. When N_p/N_j was 1/2, the eccentricity ratio was a maximum, but it did not reach unity as predicted by theory. This maximum eccentricity ratio could be lowered by increasing the speed, but it was not affected appreciably by changes in lubricant viscosity or external load. A number of theories regarding the reason for the unpredicted presence of an oil film when $N_p/N_j = 1/2$ were tested without finding any valid explanation.

Some published theoretical studies of bearings under rotating loads are based on the assumptions of constant eccentricity and constant phase angle between the line of centers and the load line. Neither of these conditions was found to exist in the test bearing.

With sinusoidal alternating loads, the orbits resembled ellipses, with the long axis in the direction of loading when N_p/N_j was greater than 1/2 and perpendicular to the load line when $1/4 < N_p/N_j < 1/2$. For values of $N_p/N_j \leq 1/4$, the paths were more complicated, the shape depending upon the particular value of N_p/N_j. These observations agree very well with Burwell's calculated findings. The major discrepancy was in the fact that, with $N_p/N_j = 1/2$, the eccentricity ratio of the orbit was less than the theoretical value of unity.

When tests were run with a combination of a rotating load at shaft speed and an alternating load at one-half shaft speed, it was found that the eccentricity ratios were not so great with the combined loads as they were with the alternating load alone. This result is pertinent to the case of crankshaft bearings in a four-stroke-cycle engine.

Battelle Memorial Institute
Columbus, Ohio, November 1, 1948

APPENDIX A

DESIGN AND CONSTRUCTION OF BEARING TESTING APPARATUS

General

A testing machine, shown photographically in figure 1, has been constructed for this investigation. The machine employs a 4-inch-diameter spindle, supported in a main bearing and a test bearing, which are both precision-bored. Lubrication is by pressure feed in circumferential oil grooves. The spindle is driven by a V-belt through a Toledo Timer speed changer. Steady, alternating, and rotating loads can be applied to the test bearing according to a selected load diagram. Measurements of the position of the center of the spindle with respect to the center of the test bearing can be made with the aid of a highly sensitive radio-frequency micrometer.

Spindle

Since the probes were designed to operate against a 4-inch-diameter measuring surface, the whole shaft was made 4 inches in diameter, thus facilitating manufacture and avoiding any errors in concentricity between the measuring section and the test section.

The shaft length was decided upon from the fact that the more the main bearing and test bearing are separated, the less pronounced would be the influence of changes in the main bearing on the measurements at the test bearing. For this reason, the shaft length was set at the comparatively large value of 28 inches.

The spindle is NE 8749 steel, normalized at 1600° F, oil-quenched from 1550° F, tempered for 24 hours at 1000° F, and furnace-cooled. This long tempering was used to reduce internal stresses and minimize the danger of warpage. The shaft was machined and finish-ground to 4.002 inches in diameter, then ring-lapped with kerosene and oleic acid, using 600-grit alundum, jeweler's emery, and levigated alumina, successively. Final polish was accomplished with 4/0 metallographic paper, wet with kerosene. No measurable out-of-roundness and a maximum variation in diameter in the entire 28-inch length of 0.00013 inch was shown by an electrolimit gage sensitive to less than 0.00001 inch. The dimensions are given in the following table.

SPINDLE DIMENSIONS

Distance from test-bearing end (in.)	Diameter (in.)	
$\frac{1}{16}$	4.00160	
$\frac{3}{8}$	4.00165	Test bearing covers journal here
$1\frac{3}{8}$	4.00165	
$2\frac{3}{8}$	4.00164	
$2\frac{3}{4}$	4.00162	
14	4.00167	
$25\frac{1}{4}$	4.00169	
$25\frac{5}{8}$	4.00171	Main bearing covers journal here
$26\frac{5}{8}$	4.00173	
$27\frac{5}{8}$	4.00173	
$27\frac{15}{16}$	4.00166	

Note that the diametral variations in the portions under the test and main bearings are only 0.00001 inch and 0.00002 inch, respectively. Consequently, it was decided to use the spindle with the dimensions shown in the table and to bore the bearings to give about the same diametral clearance in each bearing.

Test and Main Bearings

The frequently used diameter-clearance ratio of 1000 sets the diametral clearance in the two spindle bearings at 0.004 inch. In order to minimize the effect of shaft deflection on clearance, a short length-diameter ratio of 0.5 was chosen, resulting in a bearing length of 2 inches.

Originally, it was thought desirable to use a central circumferential oil groove in the test bearing, with a similar groove near each end. High-pressure oil would be introduced into the central groove, while lower-pressure oil would be supplied to the two end grooves. Such an arrangement would provide positive pressure seals at the bearing ends, thereby avoiding the entrance of air into the clearance space. Examination of this design revealed the fact that such a bearing is exactly equivalent to two end-fed bearings. Therefore, the design of the test bearing was simplified by the elimination of the central groove and the provision for independent oil-pressure controls at each end groove, resulting in a single end-fed bearing with a positive seal at each end. The main bearing was designed with a single central circumferential oil groove.

The test and main bearings are 1/4-inch-wall steel shells which were electroplated internally with 0.025 inch of pure silver and then pressed into the cast-iron housings. Silver was chosen as the material for the main and test bearings largely because of the ease with which such bearings can be made in the laboratory. Boring was accomplished in the milling machine with the aid of the precision-boring arrangement shown in figure 19. The boring bar was made of NE 8749 steel in precisely the same manner as the spindle, except that its nominal diameter was $3\frac{5}{8}$ inches instead of 4 inches. After the final ring-lapping and polishing, electrolimit-gage readings revealed no measurable out-of-roundness and a maximum variation in diameter in the entire 30-inch length of 0.00002 inch. For the boring operation, this accurately lapped boring bar was supported near each end by three pads faced with silver solder and bored to the same diameter as the boring bar. The two lower pads were bolted rigidly to the housing, while the top pad exerted a downward thrust on the boring bar through the action of a cantilever spring which connected the pad to the top of the housing. The boring bar was driven by a milling-machine spindle through a pair of universal joints. Thus, the accuracy of the bored holes was independent of errors in the milling-machine spindle and depended only on the accuracy of the boring bar.

The measured bores were as follows: Test bearing, 4.00585 inches; main bearing, 4.00630 inches.

Comparing these values with the dimensions of the spindle given in the preceding table, the diametral clearances, as determined from spindle and bearing measurements were: Test-bearing clearance, 0.00420 inch; main-bearing clearance, 0.00457 inch.

Approximately 0.010 inch of silver remained in the shells after boring. These holes, checked with a standard-bore gage, showed a maximum taper of 0.00005 inch and no measurable out-of-roundness.

After the bearings had been in service for a while, the machine was dismantled, the silver sulfide film and burs discussed in the section "Calibrations of Apparatus" were removed from the bearings, and the bores were remeasured. These measurements showed the test bearing to have a maximum diametral variation in the 2-inch length of 0.0002 inch and an out-of-roundness of 0.0003 inch, whereas the original measurements had indicated a maximum taper of 0.00005 inch and no measurable out-of-roundness. It was decided to replace this bearing with a more accurate one at a convenient stopping place in the tests (see appendix B).

Lubrication

A schematic diagram of the lubrication system is shown in figure 20. The two lubricant sources at the test bearing have independent control valves and gages, while the remainder of the bearings are supplied from a common source. The rotating-load bearing and the alternating-load bearings are supplied with lubricant from the test bearing through radial and axial oil holes in the spindle. All oil was filtered before delivery to the bearings by Purolator micronic filters.

The aspirating pump removes lubricant as it leaves the test and main bearings and thereby prevents it from running out on the spindle under the micrometer probes. A brass ring around the spindle, fastened to the bearing housing and bored about 0.001 inch larger in diameter than the bearing, forms one wall of a chamber from which the aspirator removes the lubricant. During tests with kerosene as the lubricant, it was found that the single aspirating pump could not handle the large volume of flow when the pressures at the bearings were above 15 pounds per square inch. The addition of a second aspirating pump increased this upper limit to 30 pounds per square inch.

The sump is equipped with 100 feet of 5/8-inch coiled copper tubing for water cooling, so that the oil temperature can be kept close to room temperature.

Drive

The test shaft is driven through a rubber coupling from an auxiliary shaft to avoid the transmission of vibrations. The drive is a continuously variable pulley type. The range of spindle speeds obtainable depends upon the pulleys used, and the speed can be conveniently set at any value between 150 and 3000 rpm. Most of the test work was done at spindle speeds below 1000 rpm to avoid excessive heating effects and to obtain low values of the Sommerfeld variable.

A camshaft is provided to apply rotating or alternating loads. The camshaft-drive arrangement consists of a 2:1 silent chain drive from the spindle to an intermediate shaft and a 16-pitch change-gear drive from the intermediate shaft to the camshaft. The following ratios of spindle speed to camshaft speed can be obtained: 10:1, 6:1, 4:1, 2.80:1, 2.43:1, 2.11:1, 2.06:1, 2.00:1, 1.95:1, 1.89:1, 1.65:1, 1.43:1, 1.00:1, 0.67:1, and 0.40:1.

The rotating-load jackshaft is driven from the camshaft by a 1:1 silent chain drive, including an adjustable idler sprocket to take up chain slack. With the original setup, the rotating load would turn in the opposite direction from that of the spindle. Since the majority of the work with rotating loads is planned with the load rotating in the same direction as the spindle, provision is made for accomplishing this condition by substituting a pair of 12-pitch gears for the 2:1 silent chain drive from the spindle to the intermediate shaft.

Loading Mechanism

Loads are applied, by means of compression springs, through pressure-lubricated $1\frac{1}{4}$-inch-diameter babbitt sleeve bearings. The loading springs were designed for a maximum deflection of 1 inch under a load of 500 pounds.

Alternating loads are applied by an adjustable cam, on which is mounted a ball bearing which causes the flat follower to reciprocate with simple harmonic motion as it rides on the outer race of the bearing. The eccentricity of the cam is infinitely variable between 0 and 1/2 inch (1-in. maximum follower travel). An additional spring arrangement, whereby the load on the test bearing owing to the weight of the shaft can be removed, is provided. Thus, it is possible to apply loads which vary harmonically between 0 and any desired value up to 500 pounds. It is also possible to superimpose these alternating loads upon a preset steady load.

Steady loads can be applied with the same spring by disconnecting the camshaft drive. It is also possible to run tests with suddenly applied loads by inserting a wedge between the spring housing and a nut on the loading bolt in such a manner as to transfer all load from the loading bearing to tension in the loading bolt. At the desired instant, the wedge can be driven out by a hammer blow, and the load is immediately applied to the bearing.

Rotating loads are applied through a sleeve bearing, to which is attached one arm of a bell crank. The loading spring bears on the other arm of the bell crank, which pivots on a pin through the rotating-load jackshaft.

Vibrations

The natural frequencies of the various loading springs have been calculated and were found to be safely outside the operating frequency range, as indicated in the following table.

NATURAL FREQUENCY OF LOADING SPRINGS

Spring	Natural frequency (cpm)	Operating frequency (rpm)
Steady and alternating load	4680	2000 max.
Rotating load	5000+	2000 max.

Calculations were made to determine the seriousness of angular oscillation in the coupling due to the application of an alternating load between 0 and 5000 pounds. It was found that the coupling would oscillate about 17° for each load application. To reduce this, a 100-pound, 11-inch-diameter flywheel was used, and this reduces the calculated angular fluctuation to about 2°. The entire spindle section of the machine is mounted on Goodrich Type-10 Vibro-Insulator mounts. These consist of two angles and a channel bonded together by rubber, which is stressed in shear under load. These mounts are loaded to their maximum capacity of 50 pounds per inch of length, under which condition the static deflection is 3/16 inch. The natural frequency of the mount is then 433 cycles per minute.

MEASURING SYSTEMS

Radio-Frequency Micrometer

The components of the micrometer are visible in figure 1. These consist of the receiver and power supply on the shelf at the upper left, the cathode-ray oscillograph to the right of the receiver, and the two probes, one of which is hidden from view, fastened to the test-bearing housing at an angle of 45° with the horizontal.

A description of the electrical circuits and operation of the micrometer has been published in reference 8. Briefly, minute displacements of the spindle are measured as a function of changes in electrical capacitance between the spindle and micrometer probes. This capacitance is made part of the resonant circuit of a high-frequency radio oscillator, and variations cause sufficient changes in oscillator frequency to be measured readily by techniques developed for frequency-modulation broadcasting.

Other Measurements

Load.- The test-bearing loading springs have been calibrated and fitted with direct-reading load scales with indicating pointers.

Temperature.- Bearing temperatures are measured by two iron-constantan thermocouples inserted in the test-bearing housing with junctions resting against the bearing shell. Thermocouples for lubricant-temperature measurement are inserted in wells in the feed lines just before they enter the test-bearing housing. A two-pen Bailey potentiometer continuously records the bearing and oil temperatures on a circular chart with a speed of 1 revolution in 3 hours.

Lubricant viscosity.- Temperature-viscosity characteristics of the lubricants used were determined in a modified Ubbelhode capillary viscometer immersed in a vapor bath.

Oil pressure.- All oil pressures are measured by Bourdon pressure gages. Separate gages and pressure-control valves are used for the two oil sources in the test bearing. A single gage is used for all pressure-lubricated auxiliary bearings which are fed from a manifold line on the discharge side of the pump. All three pressure gages were calibrated in a standard dead-weight tester.

Speed.- Rough observations of spindle speed are made with a stroboscopic tachometer. When the use to which the data are to be put requires more accurate determinations, a revolution counter and stop watch are used.

Spindle position.- Instantaneous and long-time measurements of the position of the center of the spindle in the clearance circle are made with the aid of the radio-frequency micrometer, described previously. The actual path of the spindle center is recorded by photographing the trace on the oscilloscope screen. Magnification is determined by direct calibration of the micrometer for a given probe setting.

CALIBRATIONS OF APPARATUS

Test-Bearing Clearance

The effective clearance in the test bearing was found by raising the spindle in its bearings by means of a cable and pulley system to which dead weights could be applied. The amount of shaft rise was measured by a Federal external comparator, graduated in 0.0001-inch divisions and readable to about one-tenth of a division, or 0.00001 inch. After each increment of dead-weight load was applied, sufficient time was allowed for the shaft to move to its new equilibrium position, and the Federal gage was read.

A plot of the lifting force applied to the spindle against the upward distance moved by the spindle is shown in figure 21. The flat portion of the curve occurred when the applied force was about 110 pounds, or approximately equal to the calculated weight of the spindle.

In order to distinguish between elastic deflections and actual movement of the spindle, the clearance was found by drawing tangents to this curve at its two extremities and measuring the distance between these two lines along the mean line of zero weight on the bearings. The clearance so found was 0.00361 inch.

The diametral clearance as determined from spindle and bearing measurements was 0.00420 inch (see section "Test and Main Bearings"). The discrepancy was later found to be caused by two things which occurred during the preliminary tests. A heavy silver sulfide film had formed on the bearing surfaces as a result of the sulfur content of the oil, and tiny burs were discovered at the edges of the oil grooves. The burs were caused by particles of grit carried by the oil in spite of thorough filtering and careful cleaning of the lines. The silver sulfide film was easily dissolved by a strong aqueous solution of sodium cyanide, and the burs were carefully removed by hand scraping. After the bearings were cleaned up, the diametral clearances along the lengths of the bearings were again determined by direct measurement. The values are listed in the following table, from which it is seen that the variation is about 4 percent in each bearing, as a result of nonuniformity of the sulfide film.

The procedure used in obtaining figure 21 was repeated after the machine was reassembled, and the clearance so found was 0.00391 inch. Since this figure was within 0.00001 inch of the minimum test-bearing clearance obtained by direct measurement (see table), it was concluded that the measurements were sufficiently accurate until the bearings could be replaced.

CLEARANCES DETERMINED BY DIRECT MEASUREMENT

Test bearing		Main bearing	
Location	Diametral clearance (in.)	Location	Diametral clearance (in.)
		Right half	
Right edge	0.00406	Right	0.00436
Right center	.00394	Center	.00435
Center	.00395	Left	.00439
Left center	.00401		
Left edge	.00392	Left half	
		Right	.00444
		Center	.00436
		Left	.00450

Dial-Gage Calibration

The micrometer probes are each mounted on a pair of cantilevers. These cantilevers are bolted together at their lower ends. One of each pair of cantilevers is very rigid, while the other is relatively flexible. The probe is attached to the rigid cantilever. A fine-pitch screw through the flexible cantilever bears on the rigid cantilever through a steel ball in the end of the screw. Tightening of the screw causes separation of the two cantilevers by bending them in opposite directions. Changes in spacing between them are measured by dial indicators graduated in 0.001-inch divisions. Thus, a large change in spacing between the two cantilevers produces a small change in position of the rigid cantilever and attached probe.

The cantilevers were calibrated by an electrolimit external comparator with the setup shown in figure 22. It was found by experiment that the 1/2-ounce pressure differential on the measuring head for full-scale deflection of the gage meter had no measurable effect on cantilever deflections. Probe movement could be read to 0.00001 inch over any

distance. Each probe was calibrated three times, with excellent duplication. Calibration curves are shown in figure 23. The slope variation in the calibration curves at high cantilever deflections is not desirable but, since it proved highly reproducible, was tolerated.

Micrometer Calibration

The electrical ciruit was then calibrated against dial-gage readings with the type of result shown in figure 24. This calibration appears to be adequately linear throughout its range.

The magnification of both probes was adjusted to be the same so that spot movement on the oscilloscope would correctly represent spindle-center movements.

APPENDIX B

TESTING-MACHINE CHANGES

Pivoted-Pad Main Bearing

In the testing machine, the precision spindle is supported at one end by the main bearing and at the other, by the test bearing. Between these two bearings, and as close as possible to the test bearing, are the probes of the radio-frequency micrometer. Originally, the main bearing was a sleeve-type bearing almost identical with the test bearing. During the course of testing, however, there appeared strong indications that the motions of the journal in the test bearing were being altered by the superimposed motions resulting from hydrodynamic action in the main bearing. These latter motions rendered precise interpretation of the micrometer oscillograms impossible and led to the substitution of a stiff pivoted-pad bearing for the large-clearance main bearing.

The pivoted-pad bearing design was based on the theory developed by Muskat, Morgan, and Meres (reference 12) for plane sliders of finite width. The error introduced by applying this theory to curved sliders was found to be relatively small. The final design consisted of four steel pivoted pads, each $1\frac{1}{2}$ inches in width by $2\frac{1}{2}$ inches arc length, faced with babbitt, and precision-bored for 0.002-inch diameteral clearance on the shaft.

The four pads shown in figure 25 were fabricated from a single hollow cylinder, babbitted internally, and rough-bored before separating. They were then assembled in the housing with tensions of 25 pounds in each adjusting spring. The adjusting screws, whose sole function was to hold the pads rigidly in position during boring, were tightened just enough to make the four pads concentric. The pivot rods had been previously lapped in their grooves. All openings between pads and housing were sealed off with masking tape to keep cutting chips out, and the pads were precision-bored by the technique described in appendix A and illustrated in figure 19.

The final bore and clearance are shown in the following table. Approximately 0.020 inch of babbitt remained on the pads after boring. The bore showed a maximum taper of 0.00005 inch and no measurable out-of-roundness.

MEASURED BEARING DIMENSIONS

Shaft diameters (measured at same time and location as bearing bore measurements):

Main-bearing end, inches 4.00102
Test-bearing end, inches 4.00100

Final bore diameter:

Main bearing, inches 4.00275
Test bearing, inches . . . . . As shown below

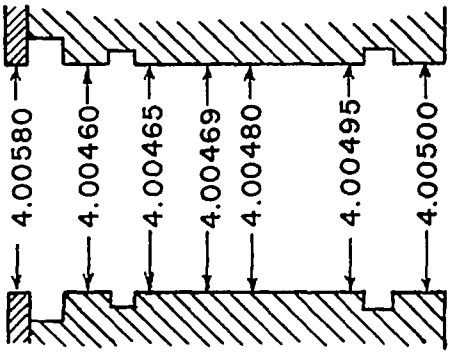

Average diametral clearance:

Main bearing, inch 0.00173
Test bearing, inch 00380

Proof of the effectiveness of this bearing in minimizing the effect of main-bearing motions on micrometer readings at the test bearing is presented in figure 26. This shows no-load starting transients under similar test conditions before and after replacement of the main bearing. The reduction of whirling motion accompanying the removal of main-bearing influences is striking.

Further evidence of the success of the pivoted-pad bearing lies in the fact that sustained whirling of the journal could not be produced in the test bearing after the pivoted-pad main bearing was installed, whereas, with the old main bearing, continuous orbital motion could be obtained under certain conditions.

By placing sensitive dial indicators in the shaft close to the two bearings and noting their range of travel when the machine was running, it was possible to ascertain the extent of whirling in the

pivoted-pad bearing. This procedure showed that this bearing was practically whirl-proof and that the amplitude of whirl at any section along the spindle length was directly proportional to the distance from the axial midpoint of the pivoted-pad main bearing. This latter observation was applied in correcting the micrometer magnification for the distance of the probe center line from the axial midpoint of the test bearing.

Attention was given to the possibility that the pivoted-pad bearing was so stiff that it limited the whirling motion in the test bearing. Evidence to the contrary was obtained from the fact that a large change in the viscosity of the lubricant in the pivoted-pad bearing had no influence on the maximum indicated eccentricities in the test bearing, as discussed in the section "Shaft rotating." Measurement of shaft stresses with strain gages near the main bearing should yield further information along this line.

Replacement of Test Bearing

While the testing machine was dismantled for replacement of the main bearing, the test bearing was also replaced. Since the stiff pivoted-pad main bearing would hold the shaft center line essentially fixed at one end, it was decided to bore the test bearing tapered in order to keep the shaft surface approximately parallel to the test bearing along the line of nearest approach. Calculations showed that the test bearing should be 0.00042 inch larger in diameter at the end farthest from the main bearing. To accomplish this and still utilize the precision-boring technique shown in figure 19, a scheme suggested by Mr. A. E. Ryder, of the Pratt & Whitney Aircraft Co., was used. In this, the tool bit was heated and therefore elongated during the process of boring.

An axial hole was drilled in a stellite tool bit and a 2-watt heating coil was cemented in with Insa-lute cement. One side of the circuit was grounded to the milling machine; a Variac provided heat control. Calibration to make the expansion linear with time and at the desired rate was done with the boring bar stationary and with the tool bit, in the bar, under the electrolimit gage.

First taper cuts in the milling machine showed the voltages indicated by static calibration to be inadequate to provide the desired taper. Voltage increases were necessary during the progress of each cut to produce a linear taper. With trial-and-error adjustments during each successive cut, the correct taper was finally achieved. As the bore approached finish size, a running electrolimit-gage check was kept on the shaft to insure accurate clearance measurements. The dimensions

of the finished test bearing are shown in the preceding table, along with shaft and pad-bearing dimensions.

Spindle and Boring Bar

The boring bar for precision boring of the main and test bearings was checked by electrolimit-gage measurements prior to the reboring operations and found to be straight and round within 0.00005-inch extreme variation. This was considered satisfactory for the reboring work, which was carried out as discussed previously.

It will be noted from the table "Spindle Dimensions" in appendix A that the spindle had a maximum diametral variation of 0.00013 inch when it was first put into service. While the machine was dismantled for repairs, it was decided to relap the spindle to decrease this variation. Ring-lapping with kerosene and 600 alundum, finishing lapping with kerosene and 1000-grit carborundum, and subsequent polishing with 4/0 metallographic paper resulted in the dimensions shown in the following table. There was no measurable out-of-roundness, and the extreme diametral variation along the entire 28-inch length was only 0.00005 inch. These measurements were made when the shaft and all measuring equipment were at a temperature of 25.4° C.

SPINDLE DIMENSIONS

Distance from shoulder at driven end of spindle (in.)	Diameter (in.)	
1/4	4.00101	Main-bearing end
1	4.00103	
2	4.00101	
4	4.00100	
6	4.00100	
8	4.00101	
10	4.00102	
12	4.00102	
14	4.00103	
16	4.00103	
18	4.00105	
20	4.00104	
22	4.00103	
24	4.00100	
26	4.00100	
27	4.00101	
$27\frac{3}{4}$	4.00100	Test-bearing end

Clearance Determination

After replacement of the main and test bearings, the clearances determined by direct shaft and bore measurements were checked by lifting the shaft in the bearings by means of a system of cables, pulleys, and dead weights. The amount of shaft rise was measured by dial gages, graduated in 0.0001-inch divisions and readable to an accuracy of about one-fourth of a division. Since the measurements of shaft rise could not be made inside the bearings, it was necessary to place the dial indicators as close as possible to the bearings and to calculate the rise at the center line of each bearing from the geometry of the system. Such calculations showed a discrepancy of about 20 percent between average clearances obtained in this manner and those listed in the table "Measured Bearing Dimensions." On the theory that the error was caused by burs from machining in the bearings, the measurements were repeated after a brief "running-in" period. This time the agreement was within 5 percent. It was concluded that the measured clearances given in the table were quite accurate, since extreme care had been taken in their determination.

It had been hoped to check the actual effective clearance in the test bearing by electrical micrometer measurements while the bearing was subjected to a cyclic load applied at one-half the frequency of spindle rotation. Theoretically, no hydrodynamic oil film can exist under such conditions, and the spindle center should trace the clearance circle. Actually, as has been discussed in this report, an oil film was found to exist, indicated by spindle-center orbits of smaller diameter than the clearance circle.

The method of locating the clearance circle on the oscilloscope screen by applying a slowly rotating load to the shaft is discussed in appendix E. Knowing the micrometer magnification, it is possible by this method to determine accurately the size and shape of the clearance circle.

Micrometer Probe Cantilevers

As can be seen from figure 23, the calibration curves of the two probe cantilevers exhibited marked departures from linearity in the high-deflection region. After a section between the bolts at the clamped ends of the cantilevers had been relieved in order to provide more positive clamping, the calibration curves, one of which is shown in figure 27, became much more linear. This linearity is desirable for accuracy and stability of calibration.

Radio-Frequency Micrometer

While the changes were being made in the testing machine, the radio-frequency micrometer was checked by plotting curves of output voltage against input frequency. These curves were nonsymmetrical and nonlinear. Furthermore, the unit was not so stable as desirable.

The limiting action of the 6AB7 limiter stage was found to be insufficient. A double limiter, using 6SJ7 tubes, was constructed. This feature made the curves of frequency against voltage output quite linear, but the output voltage swing was low. Similar results were obtained with a properly adjusted single limiter, preceded by a high-gain amplifier stage. In the final circuit, a single 6SJ7 limiter stage was preceded by a 6SJ7 amplifier stage. The plate supply voltage for the limiter stage had to be adjusted very critically to obtain proper limiting action. To obtain greater oscilloscope deflections with the low-output voltage swing available, a stable, balanced direct-current amplifier, using two 6SJ7 tubes, was built. The complete receiver circuit, after modification, is shown in figure 28.

Although this receiver was more stable and provided more linear response than any of the other circuits tried, there was still some thermal drift and nonlinearity present, as evidenced by the typical micrometer calibration curves of figure 29. If the precise size and shape of an experimentally determined orbit was desired, it was necessary to correct the oscillogram by a point-by-point process, as discussed in appendix E.

APPENDIX C

SPEED OF WHIRLING

The speed of whirling was measured by connecting one of the plates of the oscilloscope to an audio-frequency oscillator which had been carefully calibrated and tuning the oscillator to obtain a Lissajous figure, from which the frequency of whirling could be established. At frequencies too low to obtain a Lissajous figure which was stable, the frequency of whirling was established by direct counting of the rate of spot rotation. From data obtained in this manner, it was apparent that the speed of whirling was very close to half the shaft speed. However, there were small differences which might have resulted from experimental error with this type of measurement, so to determine whether the one-half ratio was exact as predicted theoretically or only approximate, as these data would indicate, another technique was adopted.

In this method, separate and accurate measurements of the shaft and the whirling velocities were not required, for the technique consisted of measuring only the departures from a precise 1:2 ratio. The technique consisted of attaching a narrow piece of adhesive tape axially on the shaft at a point where it passed under the area of measurement of the probes. Because of the different dielectric constant of the tape compared with air, there was a distinct kick on the oscilloscope screen each time the tape passed under a probe. Since the spindle rotated approximately twice for each orbital revolution, and a kick was registered for each of the two probes, the pattern on the oscilloscope screen consisted of a circle with four distinct kicks.

If the speed of the orbital rotation was precisely half the speed of shaft rotation, this pattern would not rotate at all. Any departure from this precise 1:2 ratio was indicated by slow rotation of the pattern and could be observed visually. The results obtained by this method are presented in the following table.

NO-LOAD SPINDLE-CENTER ROTATION

Spindle speed, N_j (rpm)	Oil pressures		Mean speed of spindle center in its orbit, N_e (rpm)	Ratio N_e/N_j
	Left groove (lb/sq in. gage)	Right groove (lb/sq in. gage)		
SAE 10 oil at 110° F				
826	Off	90	407.8	0.494
826	Off	80	407.8	.494
826	Off	40	407.8	.494
770	Off	80	380.4	.494
770	Off	61	380.4	.494
770	Off	50	380.4	.494
494	Off	80	244.7	.496
350	Off	80	173.6	.496
252	Off	88	125.4	.498
252	Off	78	125.4	.498
252	Off	70	125.4	.498
Straw paraffin oil at 83° F				
776	37	Off	384.7	0.496
498	37	Off	246.9	.496
350	38	Off	173.5	.496
316	38	Off	156.7	.496

From this table, it may be seen that, at a given shaft speed, the ratio of whirling frequency to shaft speed was independent of pressure in the oil grooves and that this ratio differed from a precise 1:2 by a small amount. The tests with SAE 10 oil indicated that the 1:2 ratio was approached as the shaft speed decreased. However, the results with straw paraffin oil showed no such variation but indicated the ratio was independent of shaft speed.

The possibility that the deparature from the exact 1:2 ratio of orbital speed to shaft speed was the result of small centrifugal loads on the test bearing was examined. Swift (reference 3) points out that

the ratio drops from 0.500 at zero eccentricity to 0.496 for an eccentricity ratio of 0.10. Applying these figures to the data of the table, it was found that the unbalance needed to produce an eccentricity ratio of 0.10 was far greater than any reasonable unbalance in the testing machine.

APPENDIX D

OIL-PRESSURE AND CENTRIFUGAL FORCES

Magnitudes of Forces

As mentioned in the section "Factors influencing shaft whirl," axial lubricant flow from circumferential grooves in a sleeve bearing produces Bernoulli forces which tend to decrease the eccentricity. By integrating the components of pressure over the surface of an eccentric bearing, the net centralizing force is found to be very nearly:

$$F_p = \frac{r\rho c^4(\Delta p)^2\pi\eta(4 + 3\eta^2)}{256\mu^2 w}$$

The centrifugal force on an eccentrically rotating shaft, acting in the opposite direction to increase the eccentricity, is:

$$F_c = Me(2\pi N_e)^2$$

Application to Test Bearing

The curves of figure 30 were obtained by inserting the following physical constants of the test bearing into the above equations:

$r = 5.08$ cm

$\rho = 0.86$ gram/cc (SAE 10 oil at 80° F)

$c = 0.00508$ cm

$\mu = 50 \times 10^{-5}$ gram sec/cm^2

$M = 1.7$ slugs

$N_e = \frac{1}{2}N_j$

If damping and inertia forces are ignored, the diameter of the no-load orbit described by the shaft center could be determined from

figure 30. For example, for a feed pressure of 80 pounds per square inch gage and a spindle speed of 1200 rpm, figure 30 shows that the decentralizing centrifugal force is exactly balanced by the centralizing pressure force at an eccentricity ratio of 0.50, and no-load whirling should occur at this eccentricity ratio. However, it is apparent that the damping forces would not have to be very large to upset this balance completely, since the balancing forces are only about 1/2 pound in this particular case.

Application to Gas-Turbine-Compressor Bearings

For illustrative purposes, a gas-turbine-compressor rotor, supported in two sleeve bearings having the following constants, has been assumed:

Weight of rotor - 1288 lb (644 lb per bearing)

Journal diameter - 3 in.

Rotative speed - 15,000 rpm

Radial bearing clearance - 0.0015 in.

Assuming that whirling occurs at one-half the rotor speed, the centrifugal force, for an eccentricity ratio of 1, is found to be about 1400 pounds per bearing. If the metal-to-metal friction coefficient is 0.1 and the rubbing velocity is 11,250 feet per minute, the heat generated in both bearings would be about 4000 Btu per minute or approximately 100 horsepower. There is little doubt that the bearings would fail in a short time under these conditions.

In an actual gas turbine, the severity of the conditions would be relieved somewhat by the stabilizing influences of inertia, damping, oil-pressure forces, and external loading, which have not been considered here. However, centrifugal forces have still been found sufficient to cause troublesome whirling in steam-turbine sleeve bearings.

APPENDIX E

ECCENTRICITY MEASUREMENTS

The nonlinearity of the micrometer calibration has necessitated the following somewhat involved procedure for the accurate determination of eccentricity ratios.

First, the indicated clearance circle is located on the oscilloscope screen by either photographing or plotting the observed spot movement during one cycle of application of a rotating load to the shaft, while the shaft itself is not rotating. This operation must be done very slowly to insure that no oil film will build up between the shaft and the test bearing. The closed path so obtained is then replotted on a linear rectangular coordinate system by applying micrometer calibration corrections from curves, similar to figure 29, to at least 12 points around the orbit. The resulting figure is the magnified true clearance circle. In a similar manner, any experimental spindle-center location or orbit may be corrected to its true position inside the clearance circle. The ratio of the eccentricity of any point on the corrected spindle-center path to the corresponding radius of the clearance circle is the eccentricity ratio of that point. The actual minimum oil-film thickness at that shaft-center location is merely the radial distance scaled between the point and the clearance circle.

Under certain loading conditions, it has been found that the shaft center follows a circular orbit concentric with the clearance circle. In this case, the orbit on the oscilloscope screen will have the same general shape as the indicated clearance circle, though neither will appear perfectly circular because of the nonlinear calibration. When this happens, a close approximation to the eccentricity ratio can quickly be obtained in the following manner. The photographic negative of the oscillogram of the orbit is placed in a projector and the image is projected on a screen upon which the indicated clearance circle has been drawn to scale. The distance of the projector from the screen is then adjusted until the image of the orbit coincides exactly with the drawing of the indicated clearance circle on the screen. The ratio of the magnification of the indicated clearance circle to the magnification of the superimposed orbit on the screen then gives the eccentricity ratio directly.

It may be seen from figure 29 that the micrometer calibration was sufficiently linear that direct measurements of eccentricity, based on an average micrometer magnification, were accurate enough for comparative studies and for indicating trends. However, when more precise

eccentricity measurements were desired, the first method discussed was used. Taking into account the accuracy with which linear measurements could be made from the photographs, the reported values of η are subject to errors of about ± 0.01.

REFERENCES

1. Harrison, W. J.: The Hydrodynamical Theory of the Lubrication of a Cylindrical Bearing under Variable Load, and of a Pivot Bearing. Trans. Cambridge Phil. Soc., vol. 22, Feb. 1920, pp. 373-388.

2. Robertson, D.: Whirling of a Journal in a Sleeve Bearing. Phil. Mag., ser. 7, vol. 15, no. 96, Jan. 1933, pp. 113-130.

3. Swift, H. W.: Fluctuating Loads in Sleeve Bearings. Jour. Inst. Civ. Eng., no. 4, 1936-37, pp. 161-195.

4. Bell, J. C.: Note on the Hydrodynamic Theory of Journal Bearings. Abstract, Phys. Rev., vol. 68, nos. 3 and 4, second ser., Aug. 1 and 15, 1945, pp. 101-102.

5. Frankel, A.: Calculation of the Performance Characteristics of Plain Bearings. The Engineers' Digest (Am. Ed.), vol. 3, no. 5, May 1946, pp. 223-228; vol. 3, no. 6, June 1946, pp. 287-290; vol. 3, no. 8, Aug. 1946, pp. 400-403; vol. 3, no. 9, Sept. 1946, pp. 465-468.

6. Dick, J.: Alternating Loads on Sleeve Bearings. Phil. Mag., ser. 7, vol. 35, no. 251, Dec. 1944, pp. 841-848.

7. Burwell, J. T.: The Calculated Performance of Dynamically Loaded Sleeve Bearings. Jour. Appl. Mech., vol. 14, no. 3, Sept. 1947, pp. A-231 - A-245.

8. Foley, G. M.: Testing of Precision-Lathe Spindles. Trans. A.S.M.E., vol. 67, no. 7, Oct. 1945, pp. 553-556.

9. Hagg, A. C.: The Influence of Oil-Film Journal Bearings on the Stability of Rotating Machines. Jour. Appl. Mech., vol. 13, no. 3, Sept. 1946, pp. A-211 - A-220.

10. Muskat, M., and Morgan, F.: The Thick-Film Lubrication of Full Journal Bearings of Finite Width. Jour. Appl. Mech., vol. 6, no. 3, Sept. 1939, pp. A-117 - A-121.

11. Underwood, A. F., and Stone, J. M.: Load-Carrying Capacity of Journal Bearings. SAE Quart. Trans., vol. 1, Jan. 1947, pp. 56-67.

12. Muskat, M., Morgan, F., and Meres, M. W.: Studies in Lubrication - Part VII. The Lubrication of Plane Sliders of Finite Width. Jour. Appl. Phys., vol. II, no. 3, March 1940, pp. 208-219.

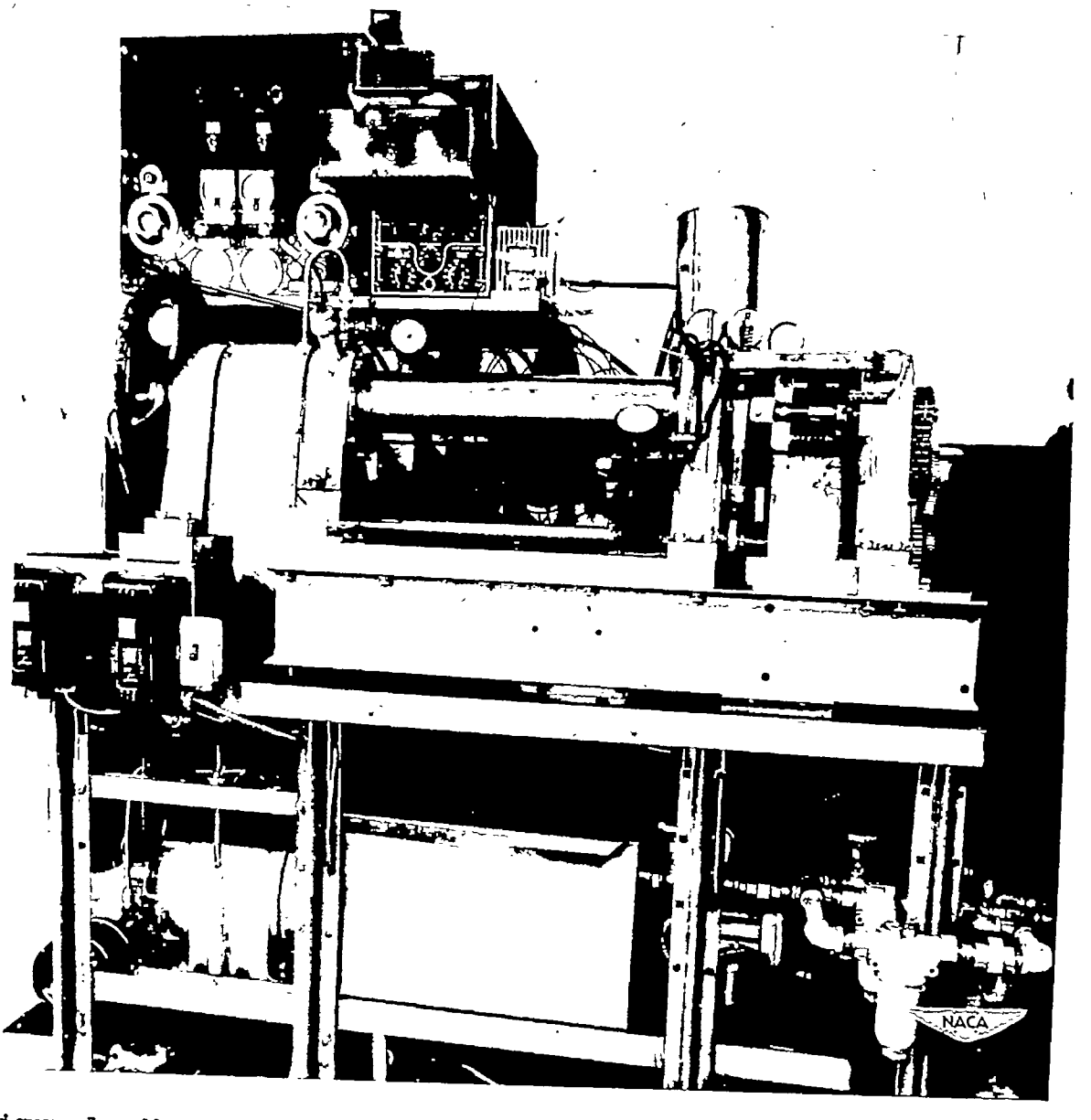

Figure 1.- Machine for testing hydrodynamically lubricated sleeve bearings under various loading conditions.

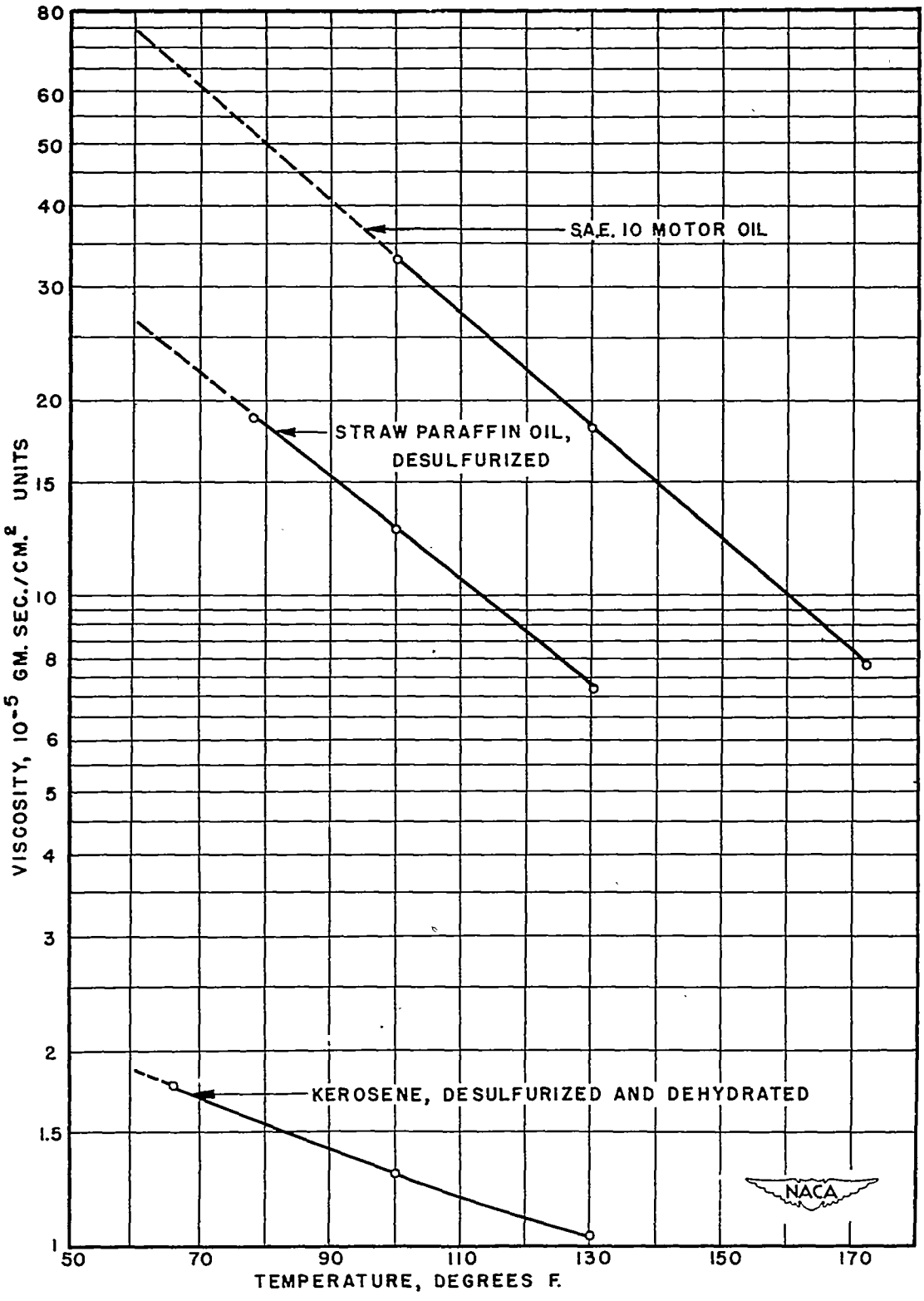

Figure 2.- Temperature-viscosity characteristics of test lubricants.

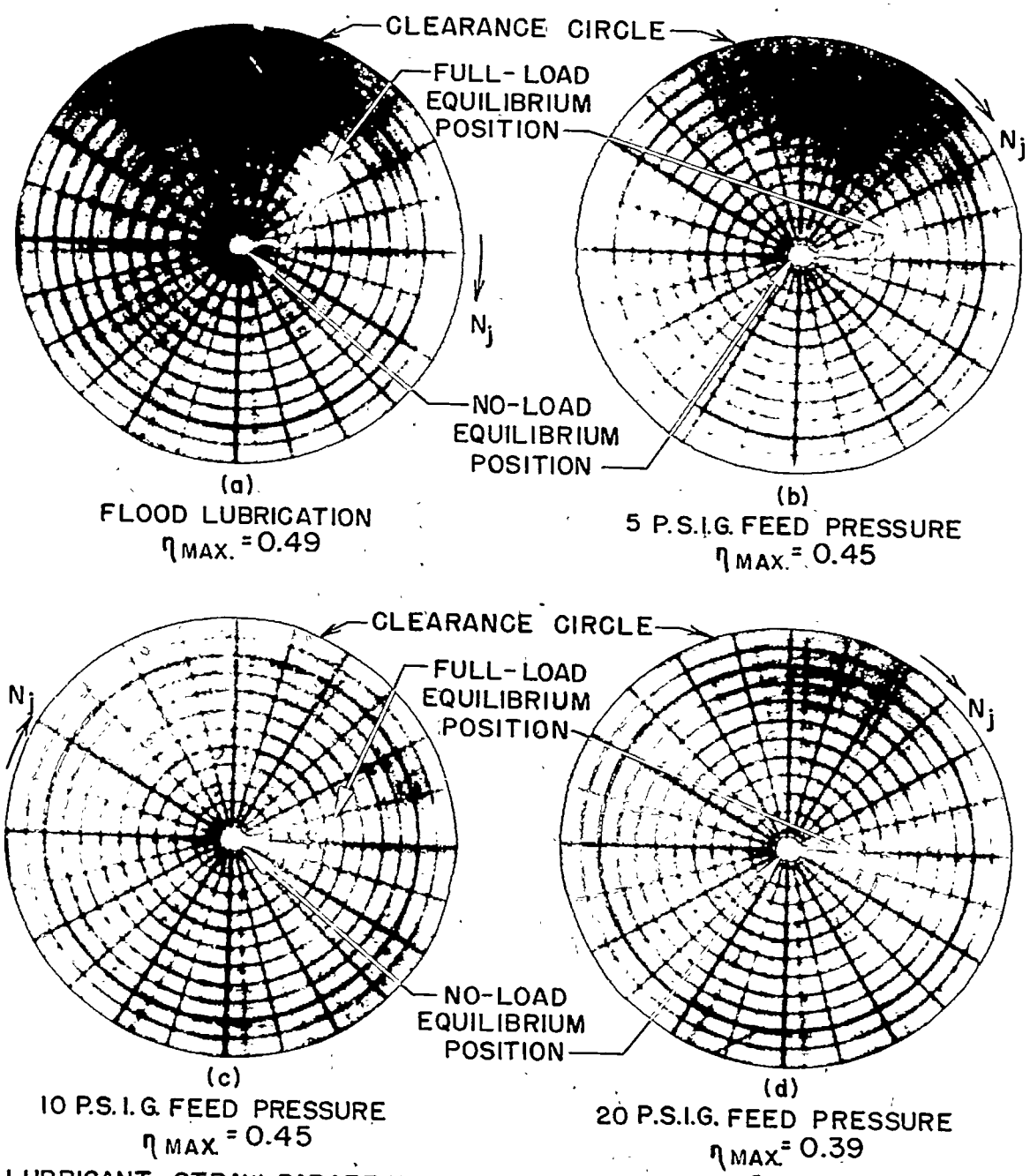

LUBRICANT-STRAW PARAFFIN OIL AT 75°F ($\mu = 20.0 \times 10^{-5}$ GM. SEC./CM.^{2})
SPEED - 600 R.P.M.
UPWARD LOAD-ZERO TO 50 P.S.I., GRADUALLY APPLIED
$S_{MIN.} = 0.529$

Figure 3.- Effect of feed pressure on shaft position. X690.

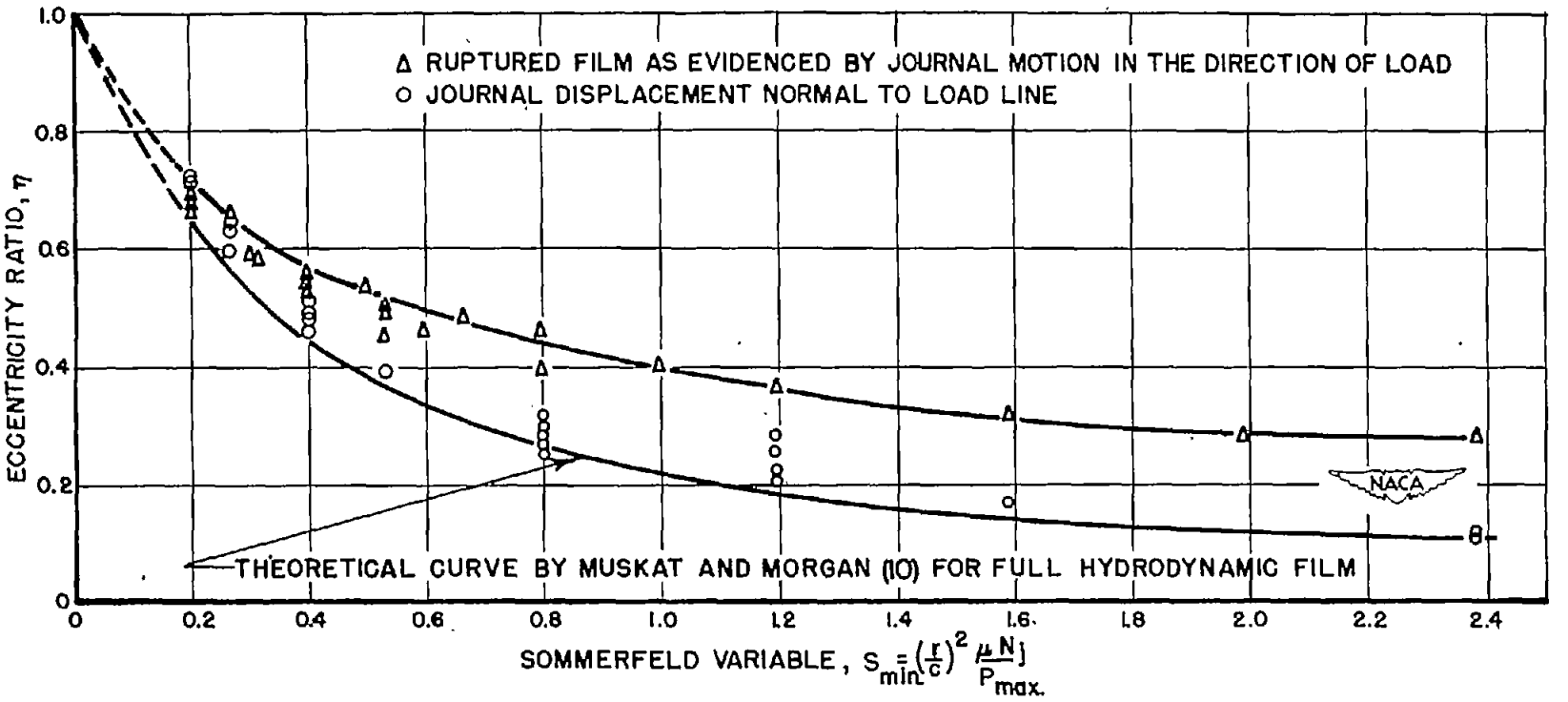

Figure 4.- Observed eccentricity of test bearing.

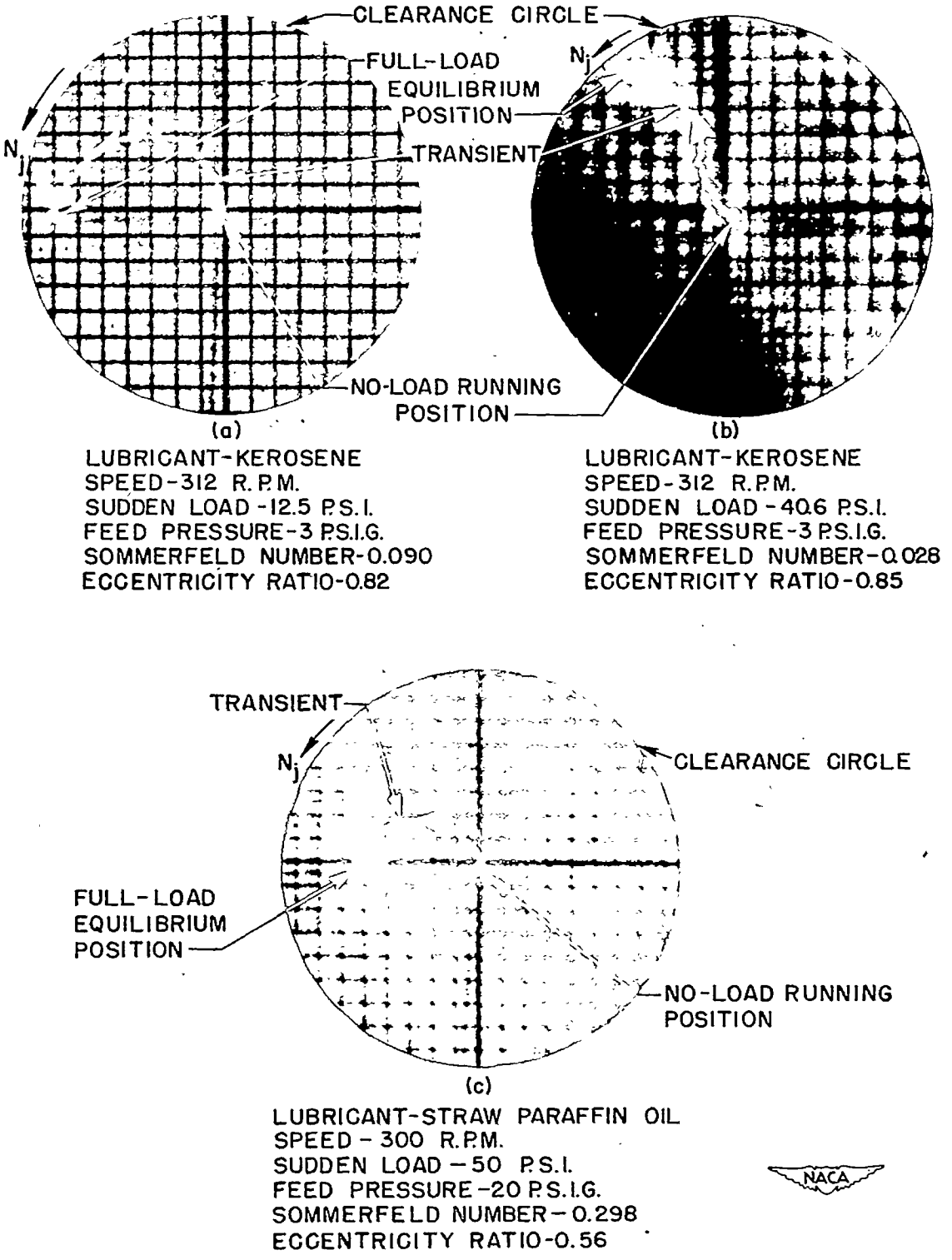

Figure 5.- Spindle motions under suddenly applied upward load. X665.

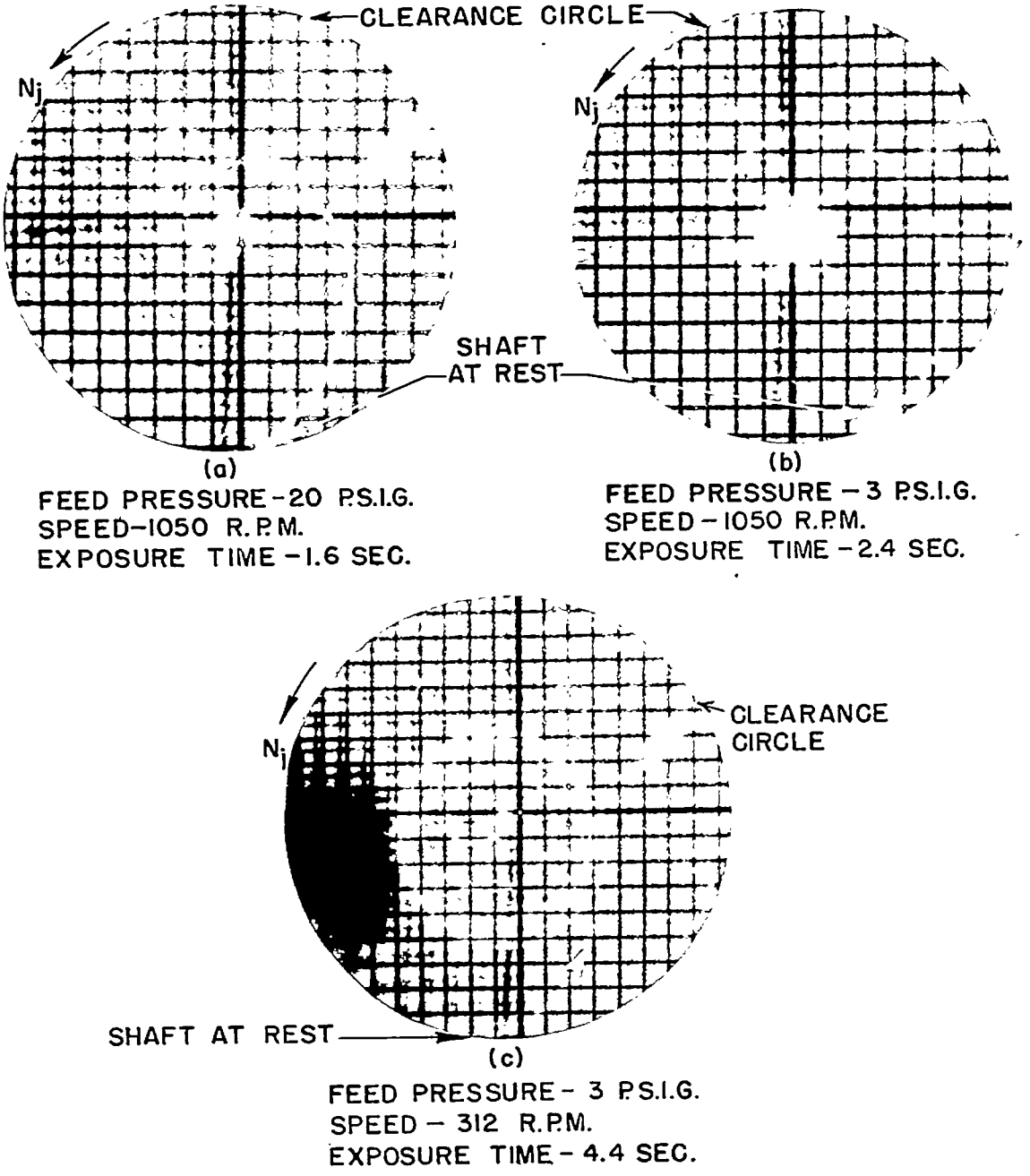

Figure 6.- No-load starting transients using kerosene at 80° F as lubricant. X700.

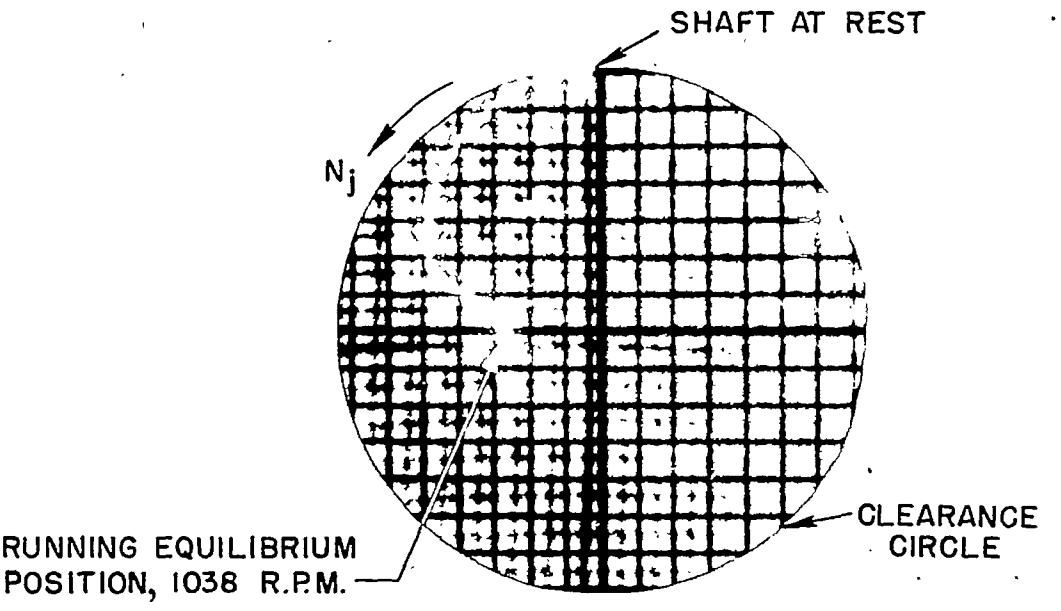

SOMMERFELD VARIABLE AT EQUILIBRIUM = 0.752
EXPOSURE TIME = 1.3 SEC.
LUBRICANT – STRAW PARAFFIN OIL

Figure 7.- Starting transient under upward load of 50 pounds per square inch. X740.

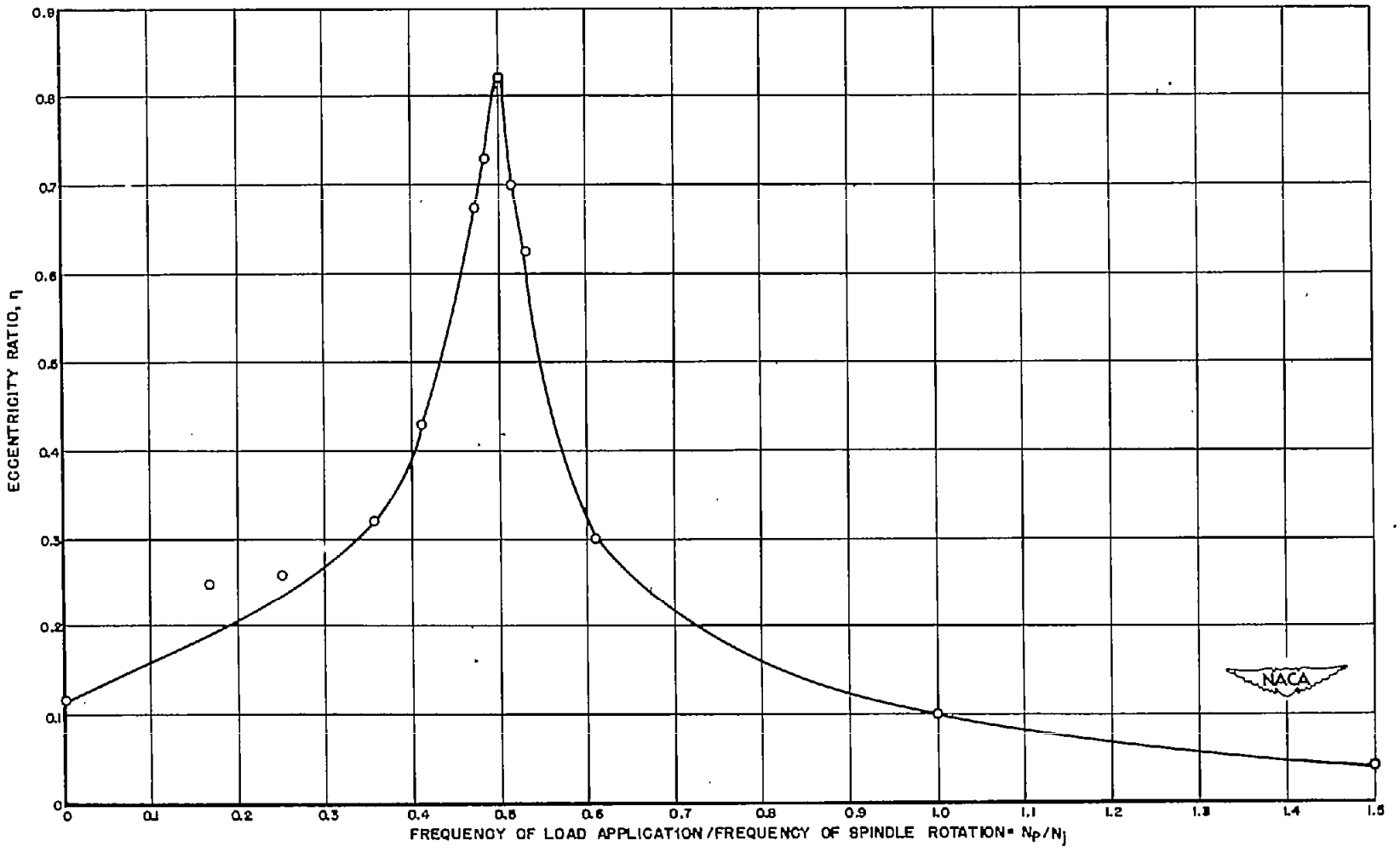

Figure 8.- Effect of relative frequency of load application on eccentricity ratio for constant load of 7.8 pounds per square inch rotating at constant speed. S = 2.38.

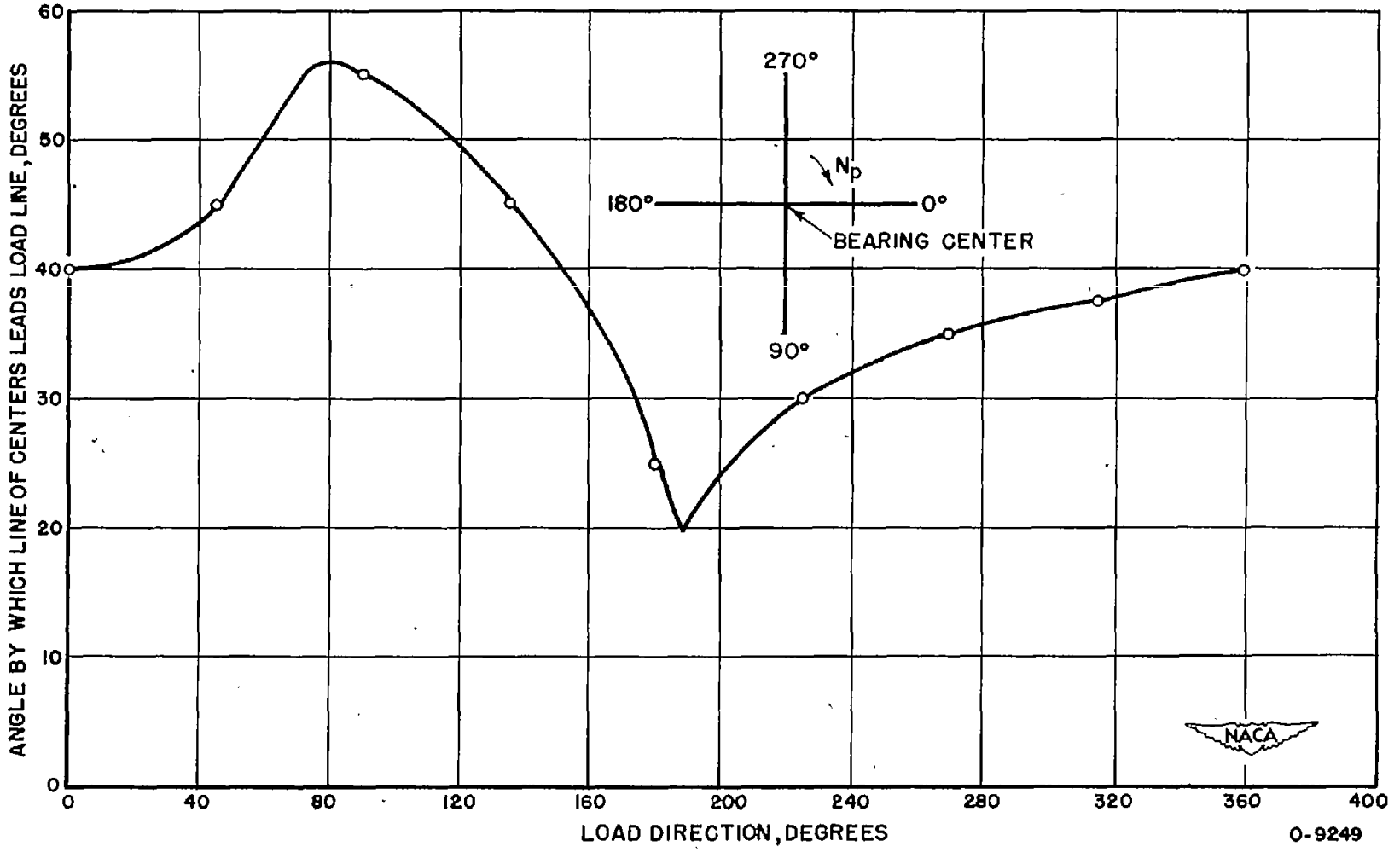

Figure 9.- Variation in phase angle between line of centers and load line for one cycle of load application with 12.5-pound-per-square-inch load rotating at one-sixth shaft speed. Shaft speed, 150 rpm; lubricant, SAE 10 oil at 81° F; flood lubrication.

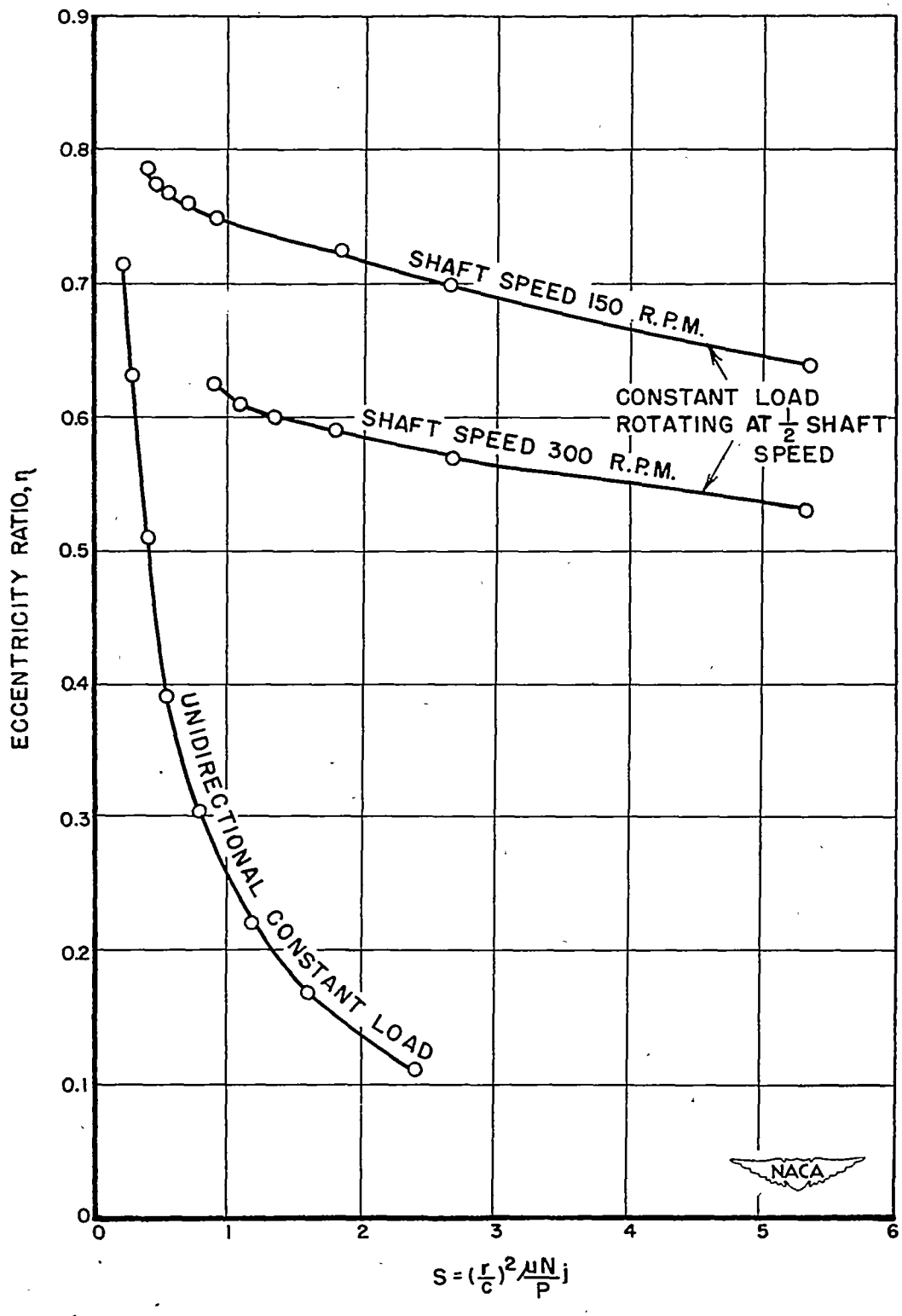

Figure 10.- Eccentricity measurements for constant load rotating at one-half shaft speed. Flood lubrication with straw paraffin oil.

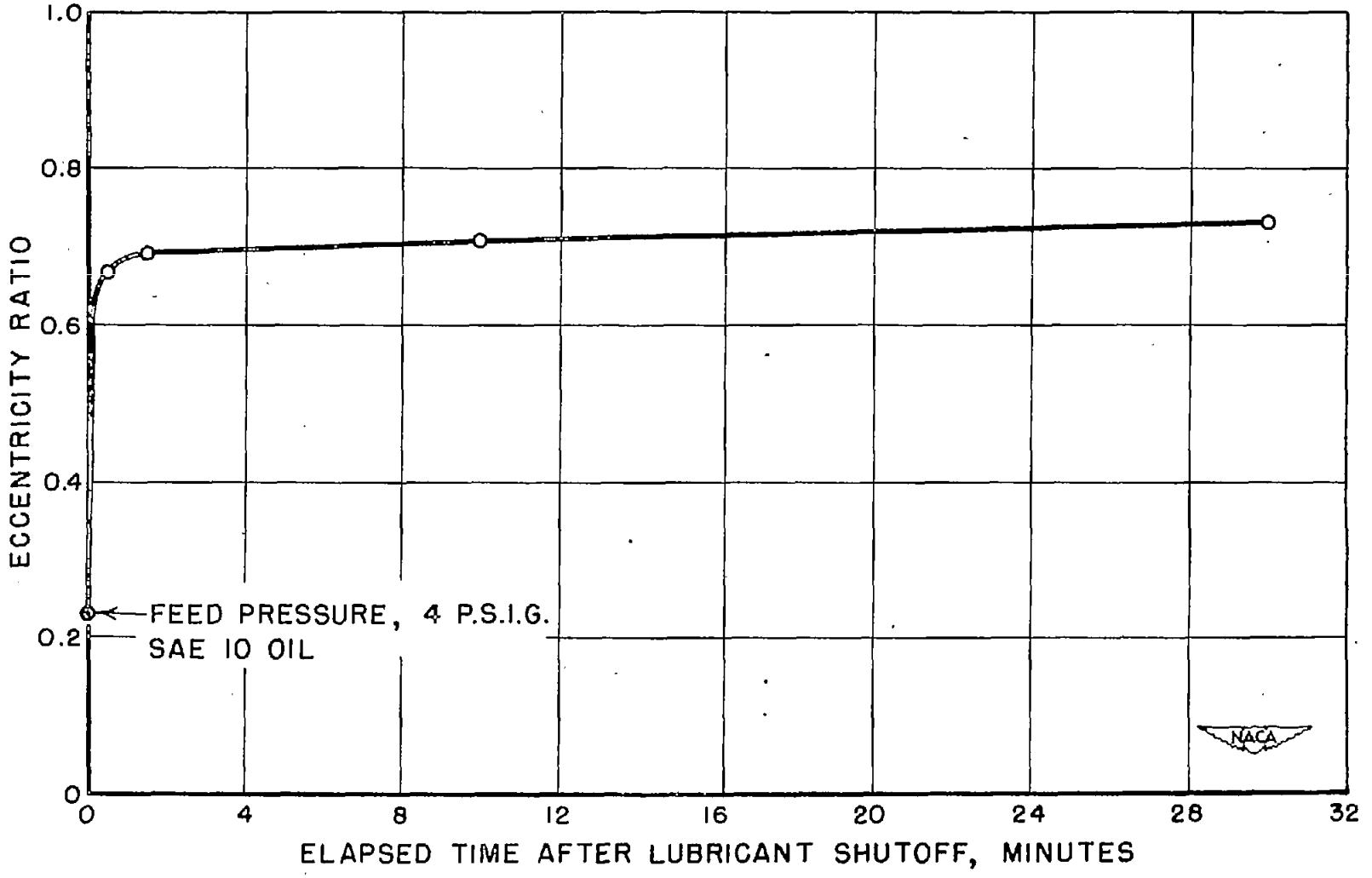

Figure 11.- Changes in eccentricity after lubricant supply cut-off. Shaft stationary; 25-pound-per-square-inch load rotating at 97 rpm.

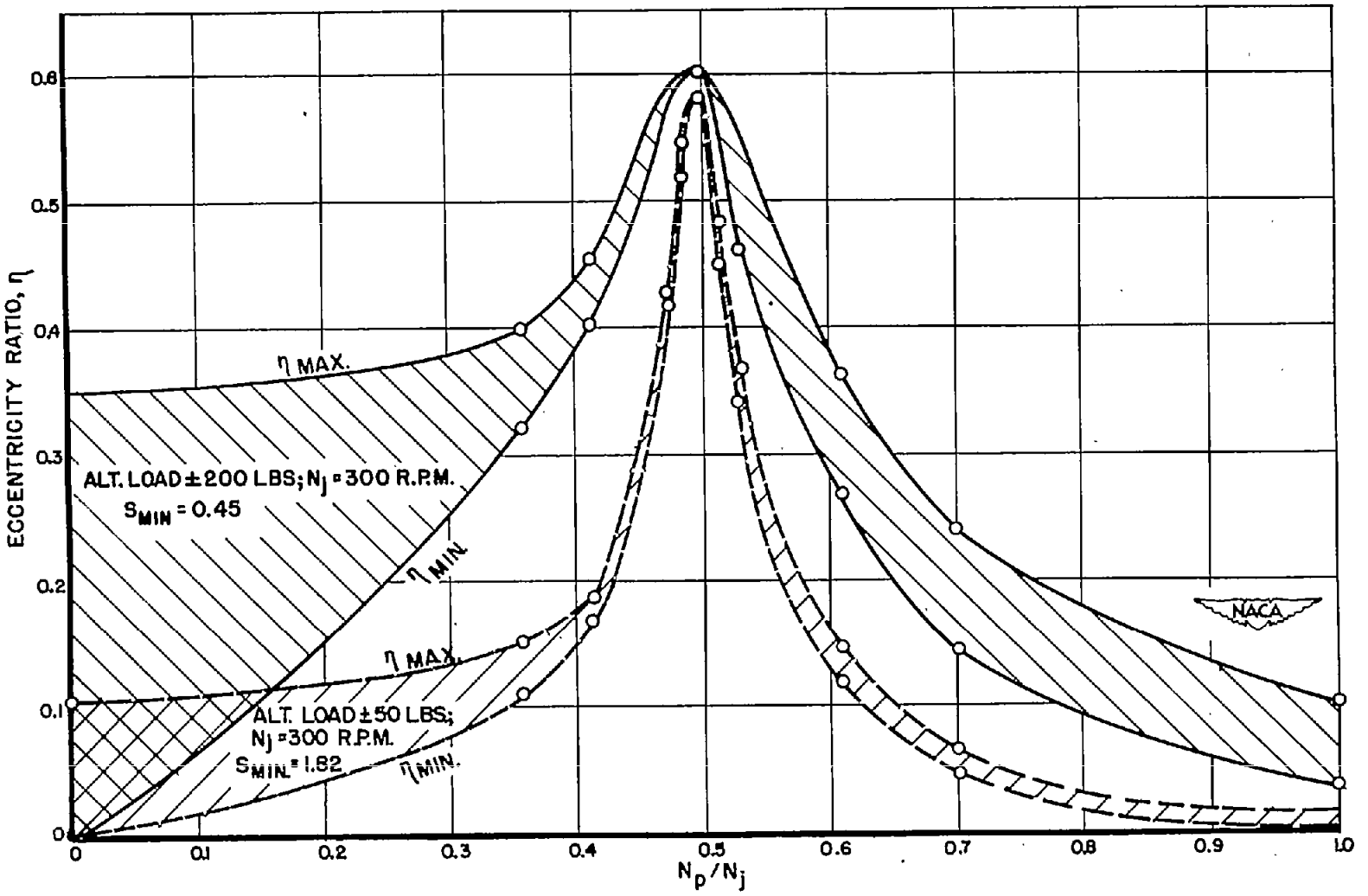

Figure 12.- Shaft motions in journal bearing with sinusoidal loads at various frequencies.

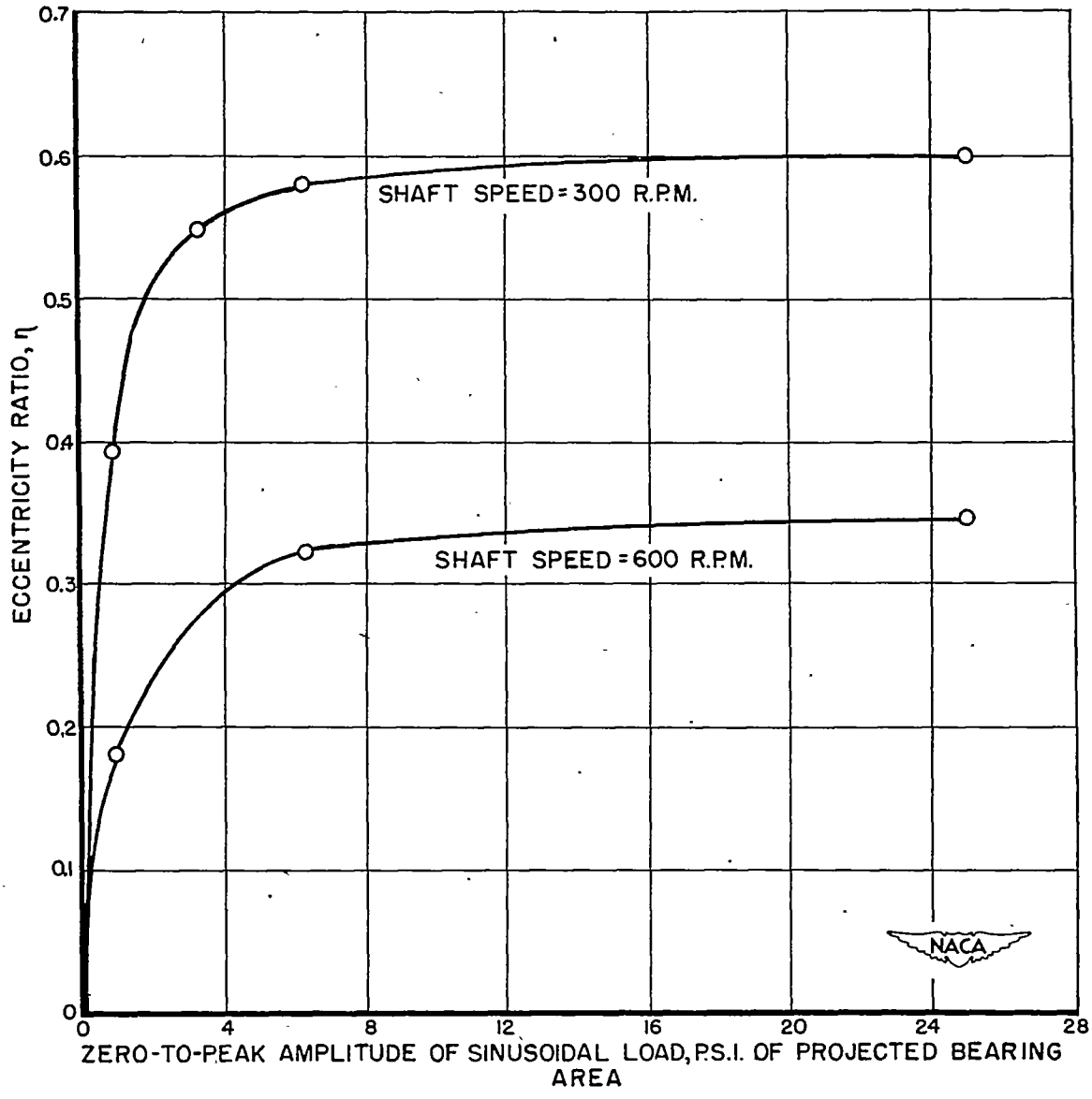

Figure 13.- Effect of magnitude of load on eccentricity for sinusoidal loading at one-half frequency of shaft rotation.

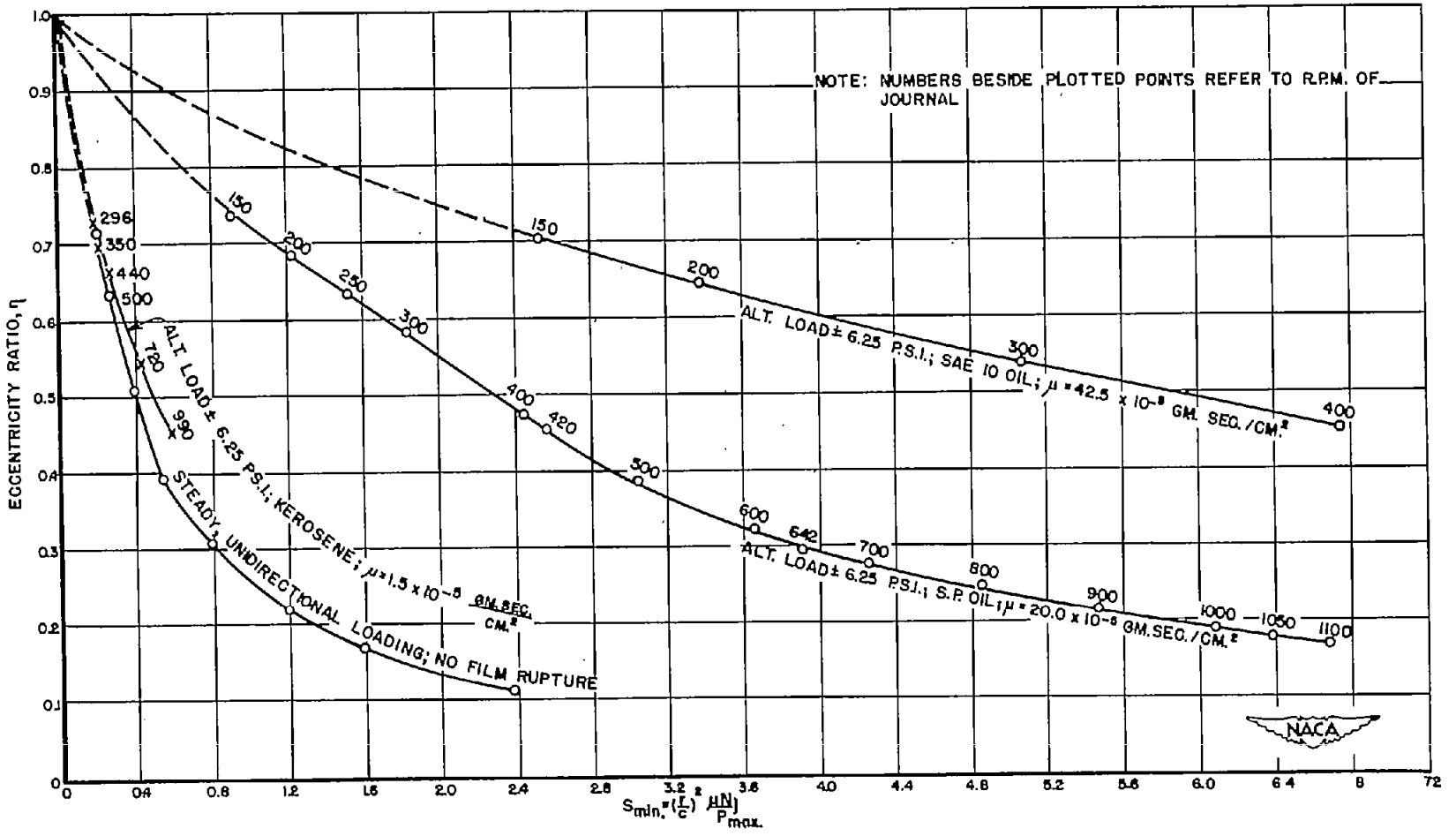

Figure 14.- Eccentricity with sinusoidal loading at one-half frequency of journal rotation $\left(N_p = \frac{1}{2} N_j\right)$.

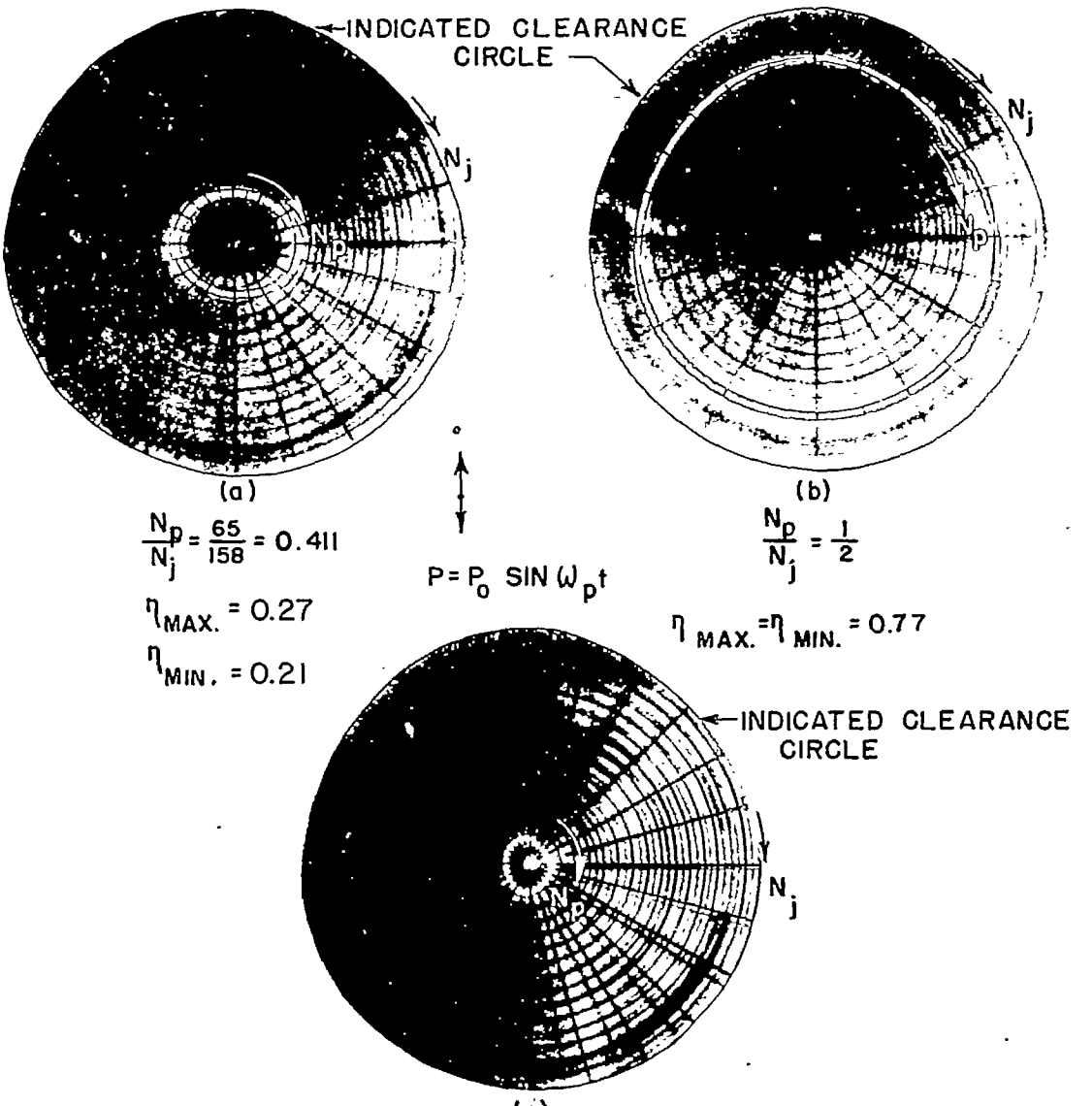

LUBRICANT-S.A.E. 10 OIL AT 80°F. ($\mu = 50.0 \times 10^{-5}$ GM.SEC./CM.^{2})
SPEED – N_j = 150 R.P.M.
PEAK LOAD – $P_o = \pm 7.8$ P.S.I.
$S_{MIN.} = \left(\frac{r}{c}\right)^2 \frac{\mu N_j}{P_o} = 2.38$

Figure 15.- Path of journal center under sinusoidal alternating load. X660.

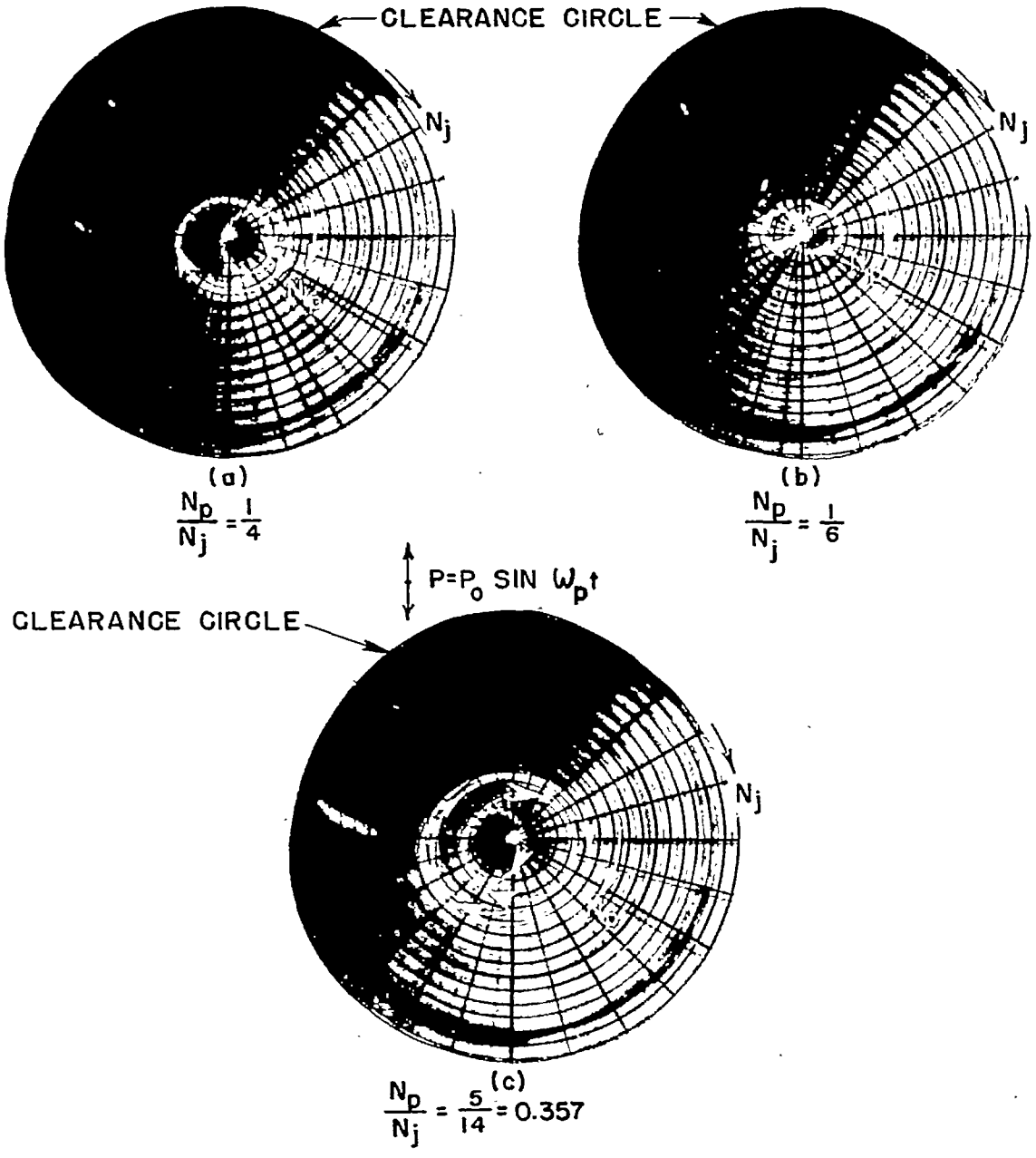

LUBRICANT - S.A.E. 10 OIL AT 80°F. ($\mu = 50.0 \times 10^{-5}$ GM. SEC./CM.^{2})
SPEED - N_j = 150 R.P.M.
PEAK LOAD - $P_o = \pm 7.8$ P.S.I.
$S_{MIN.} = \left(\frac{r}{c}\right)^2 \frac{\mu N_j}{P_o} = 2.38$

Figure 16.- Journal-center path under sinusoidal alternating load. X710.

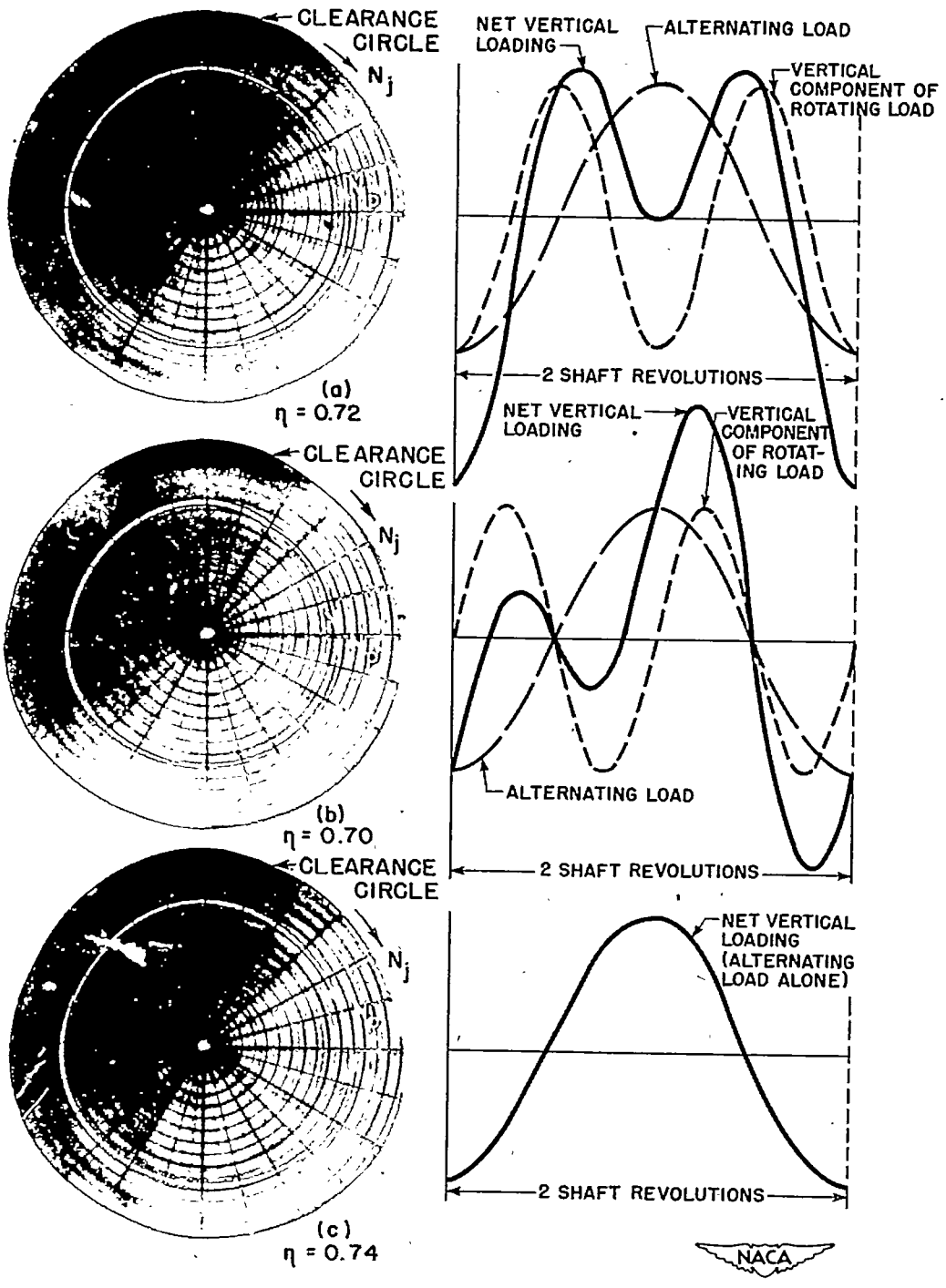

Figure 17.- Journal-center motions under combined sinusoidal alternating and constant rotating loads. Alternating load, ±12.5 pounds per square inch at one-half shaft speed; rotating load, 12.5 pounds per square inch at same speed as shaft; lubricant, SAE 10 oil at 83° F; shaft speed, 150 rpm; X600.

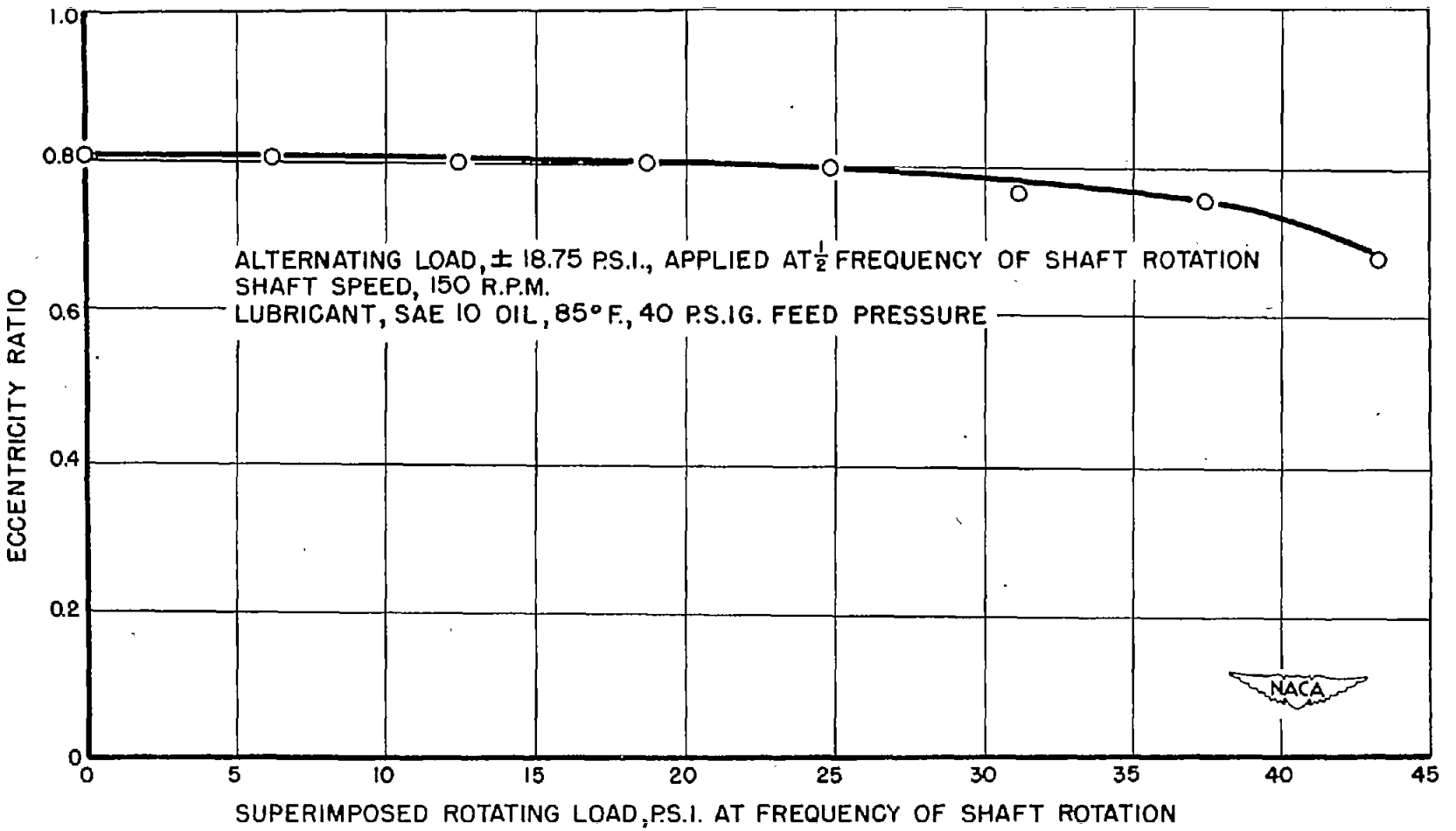

Figure 18.- Eccentricity under combined periodic loads.

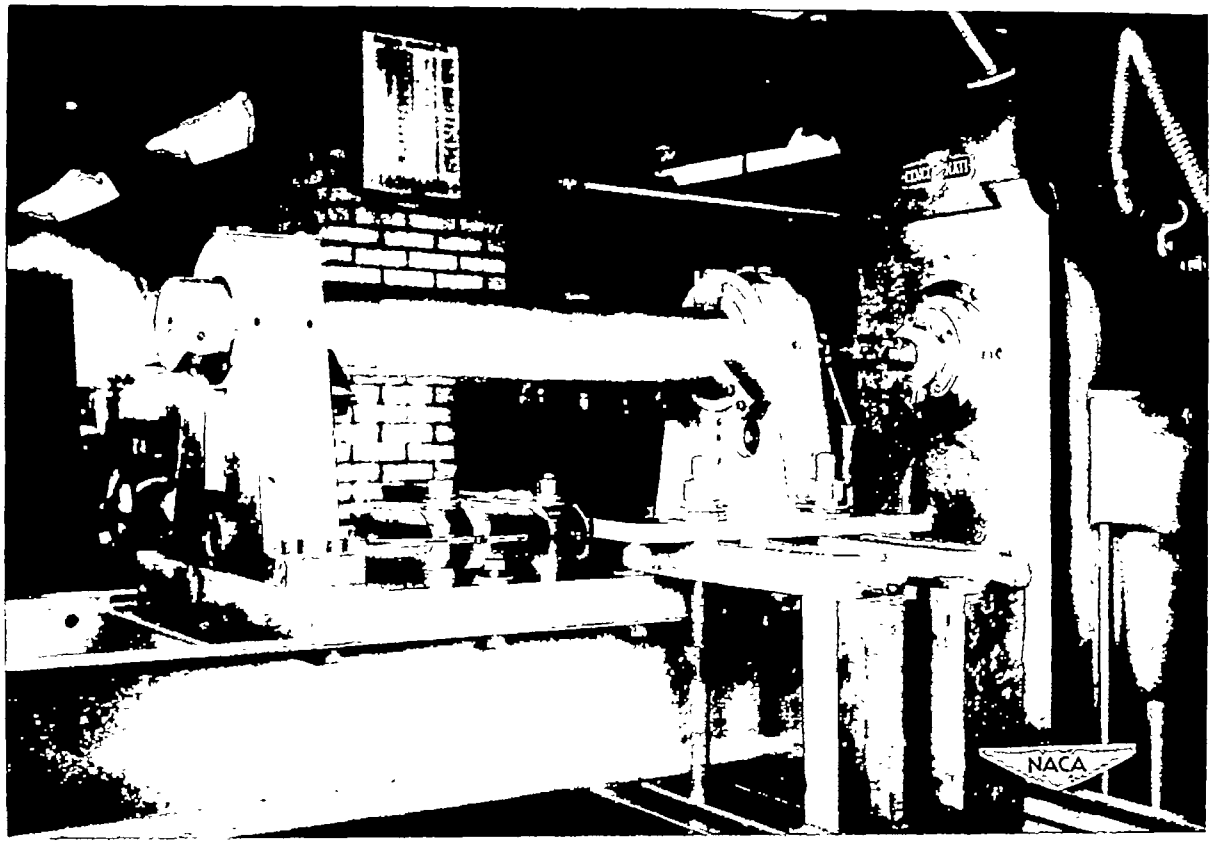

Figure 19.- Precision-boring arrangement for test and main bearings.

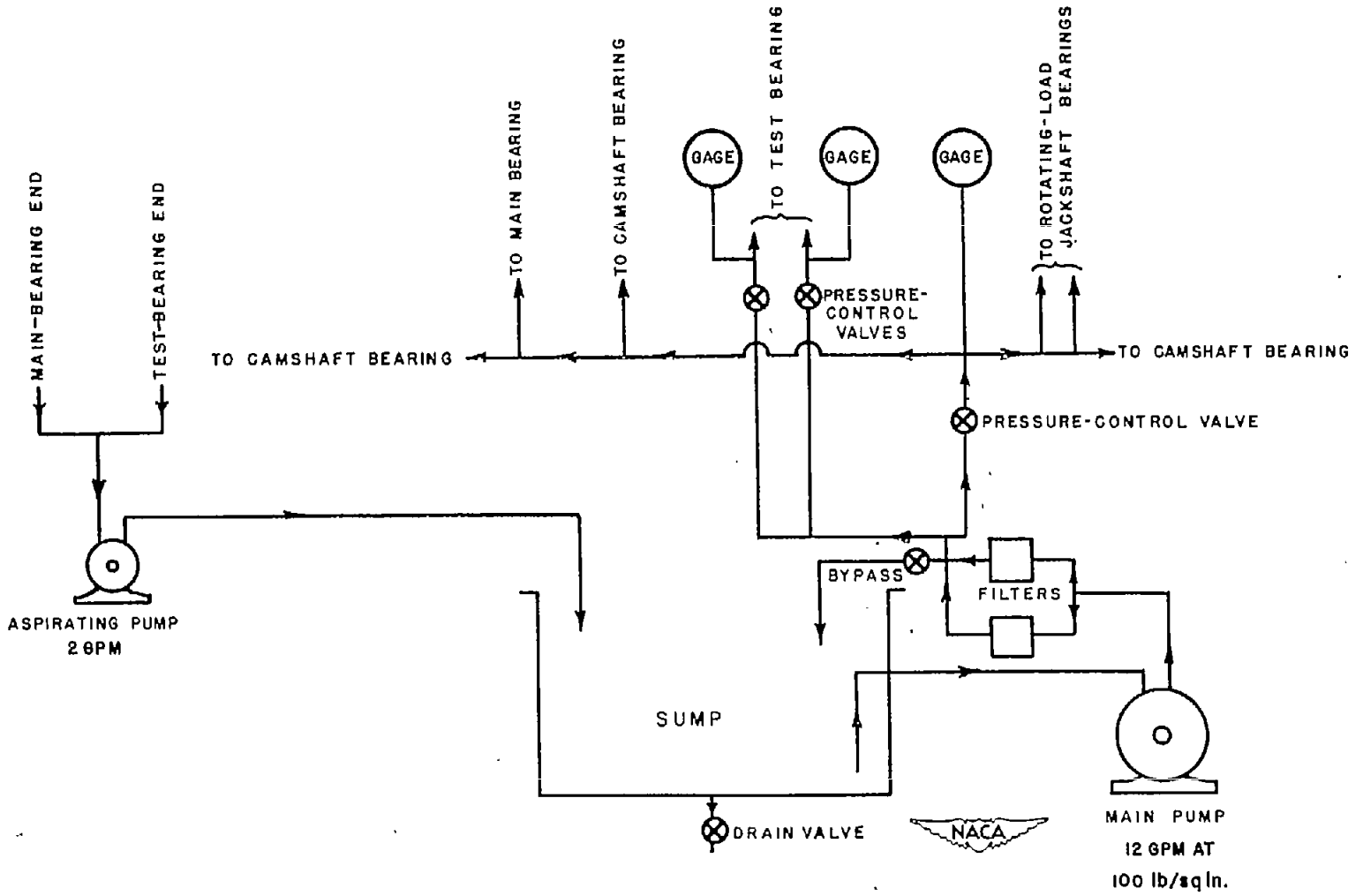

Figure 20.- Schematic diagram of lubrication system.

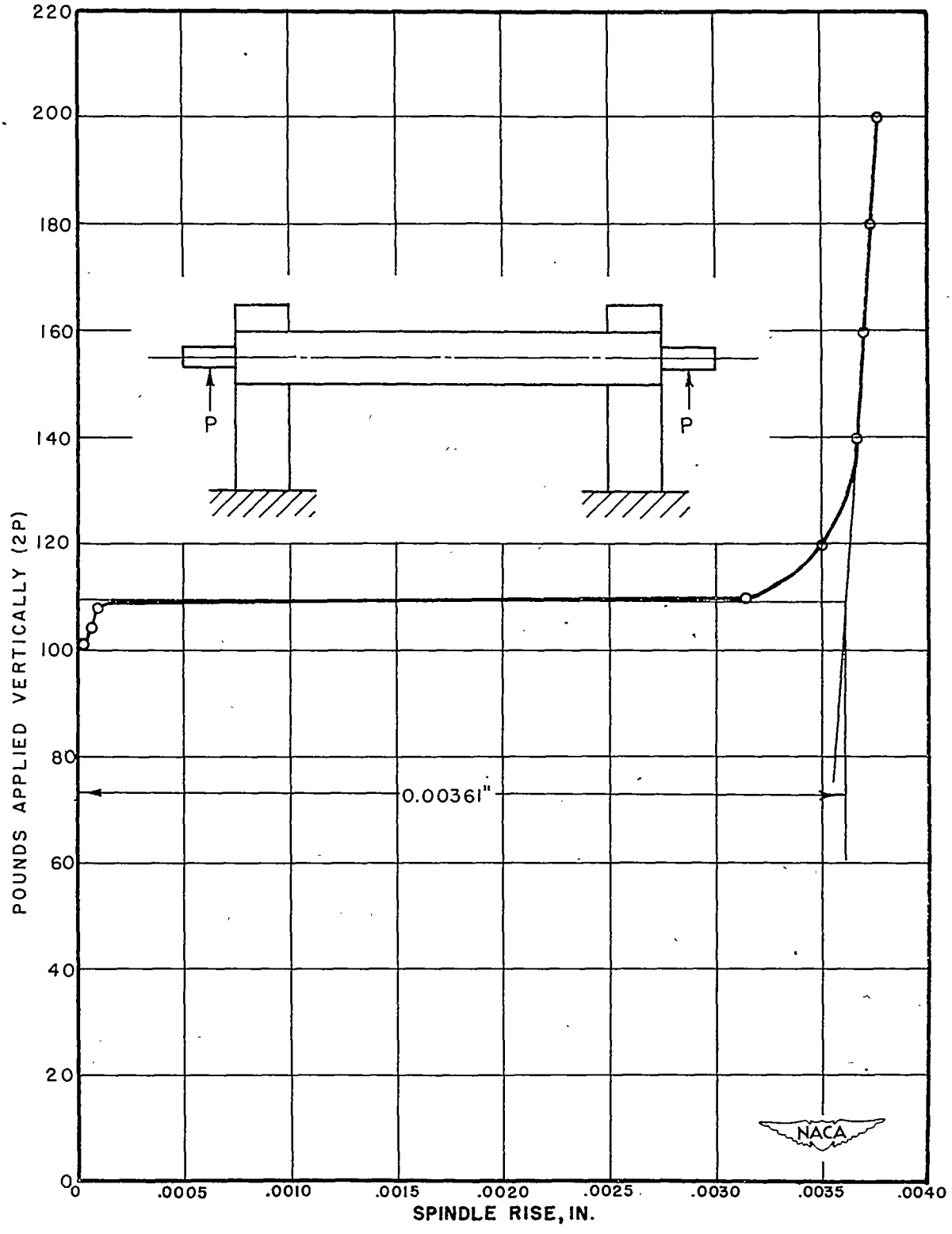

Figure 21.- Spindle clearance diagram.

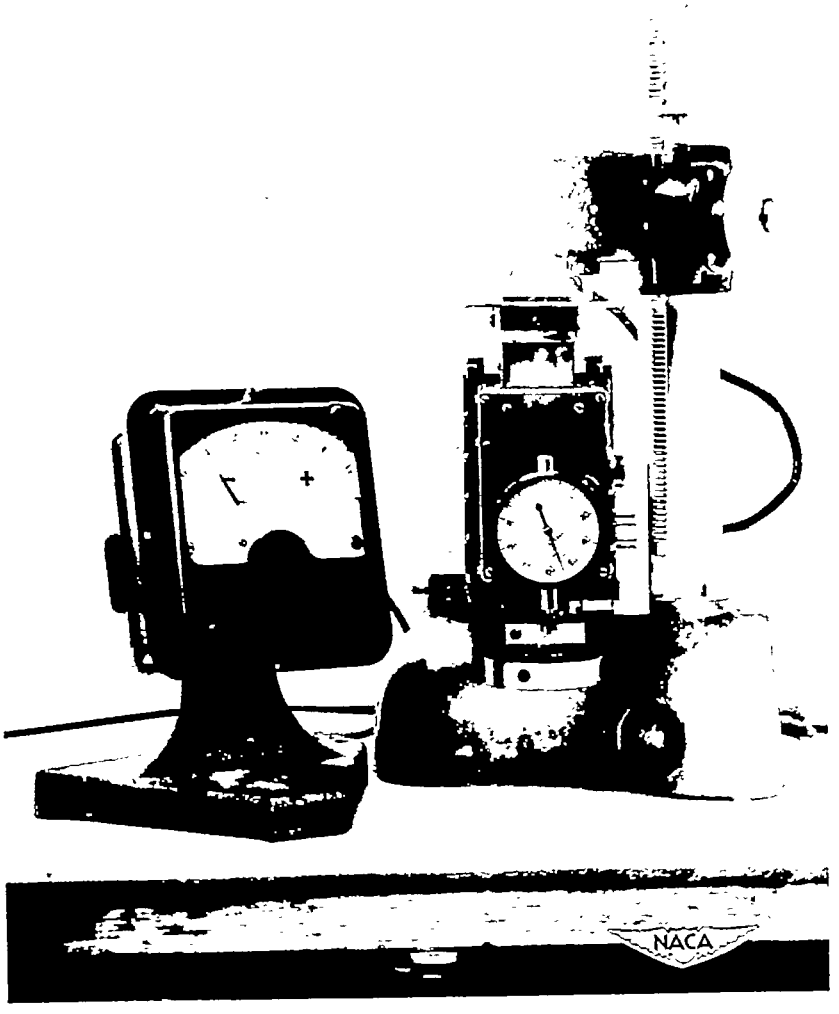

Figure 22.- Equipment for calibration of cantilevers.

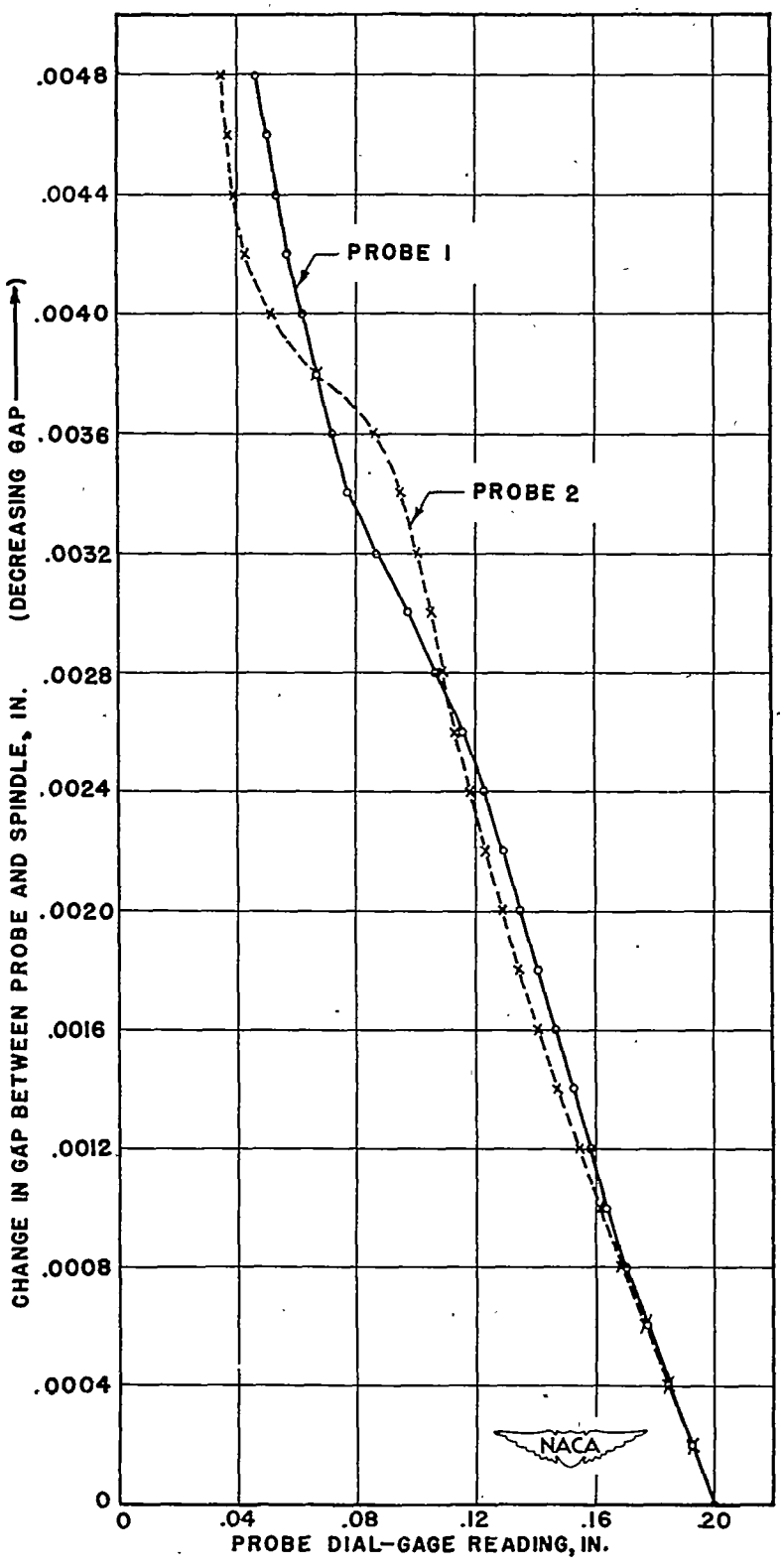

Figure 23.- Calibration of probe cantilevers.

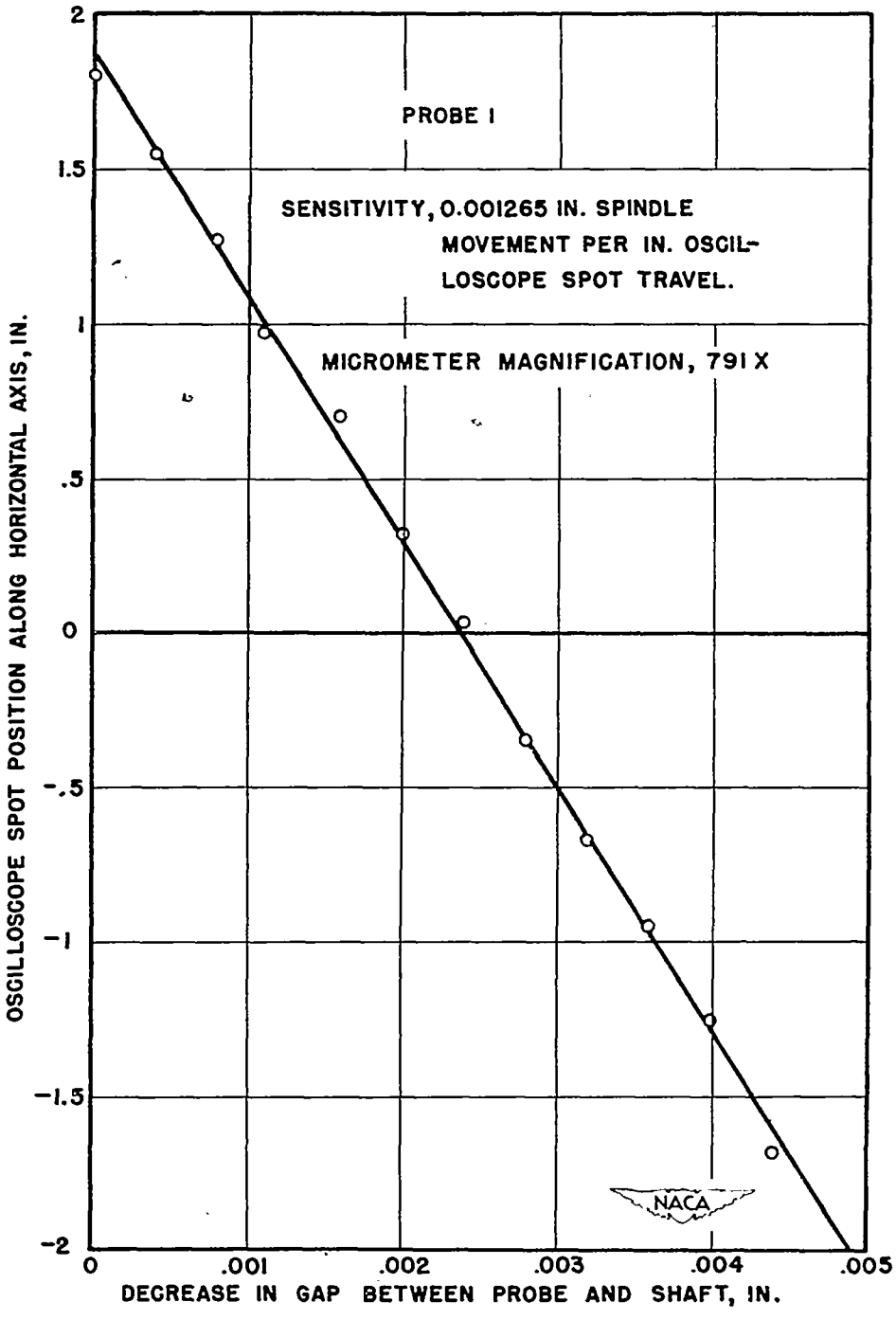

Figure 24.- Typical calibration curve for radio-frequency micrometer.

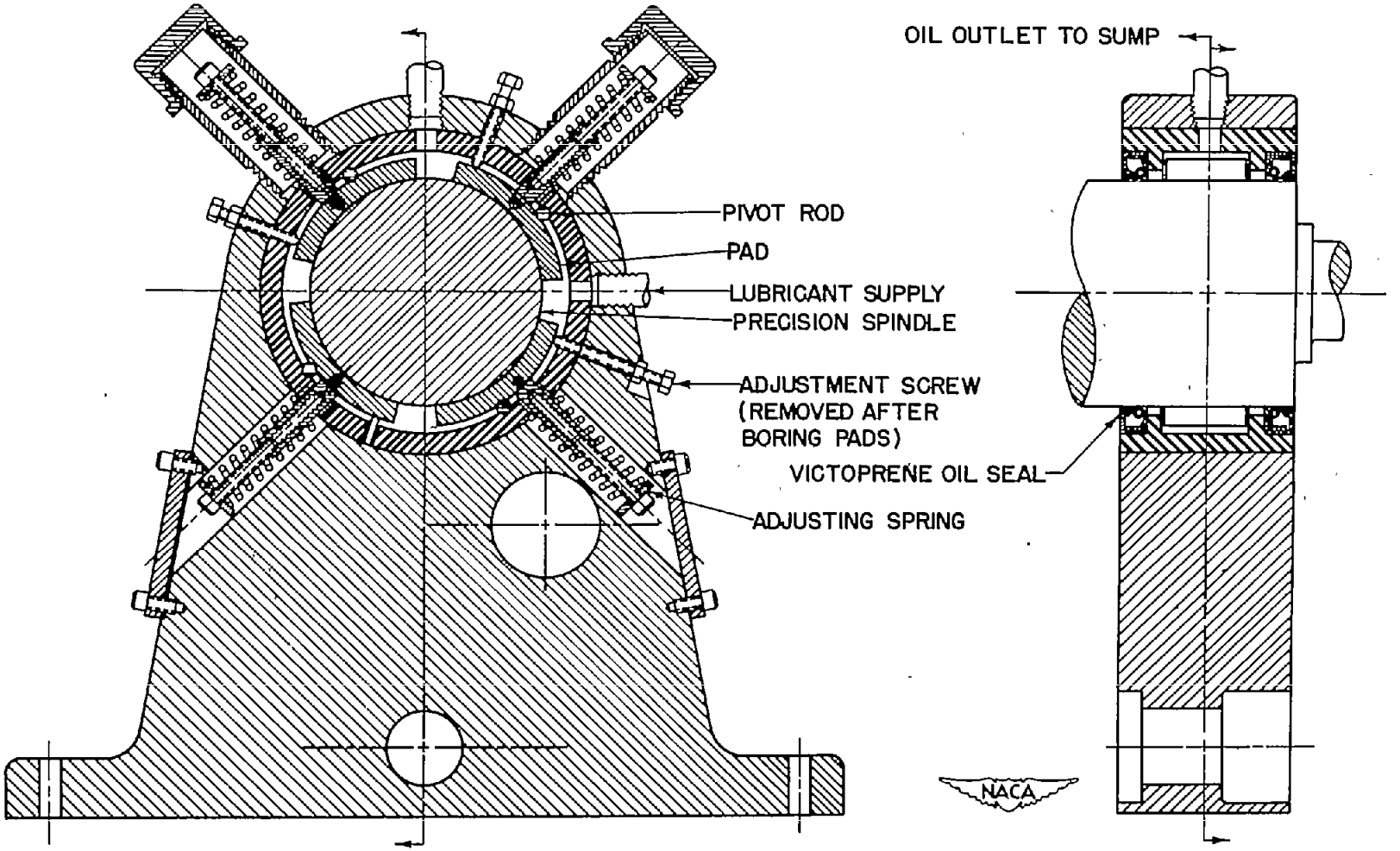

Figure 25.- Pivoted-pad main bearing.

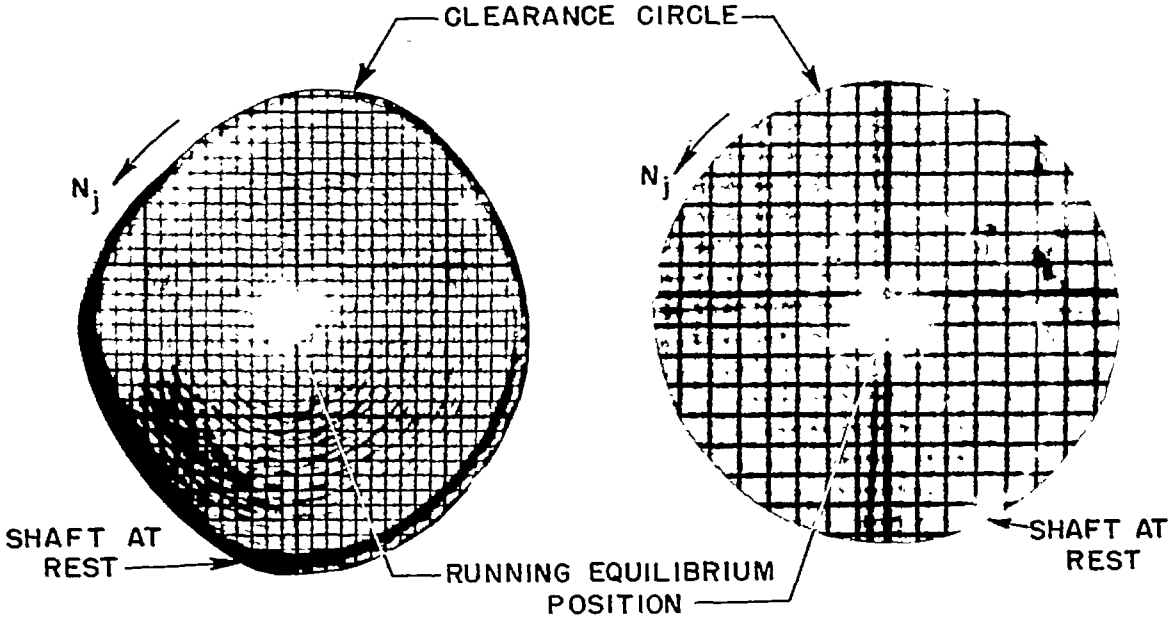

(a) With sleeve-type main bearing. Speed, 960 rpm; feed pressure, 4 pounds per square inch gage; exposure time, 15 seconds.

(b) After replacement of sleeve-type main bearing by pivoted-pad bearing. Speed, 1050 rpm; feed pressure, 3 pounds per square inch gage; exposure time, 2.4 seconds.

Figure 26.- No-load starting transients using kerosene as lubricant.

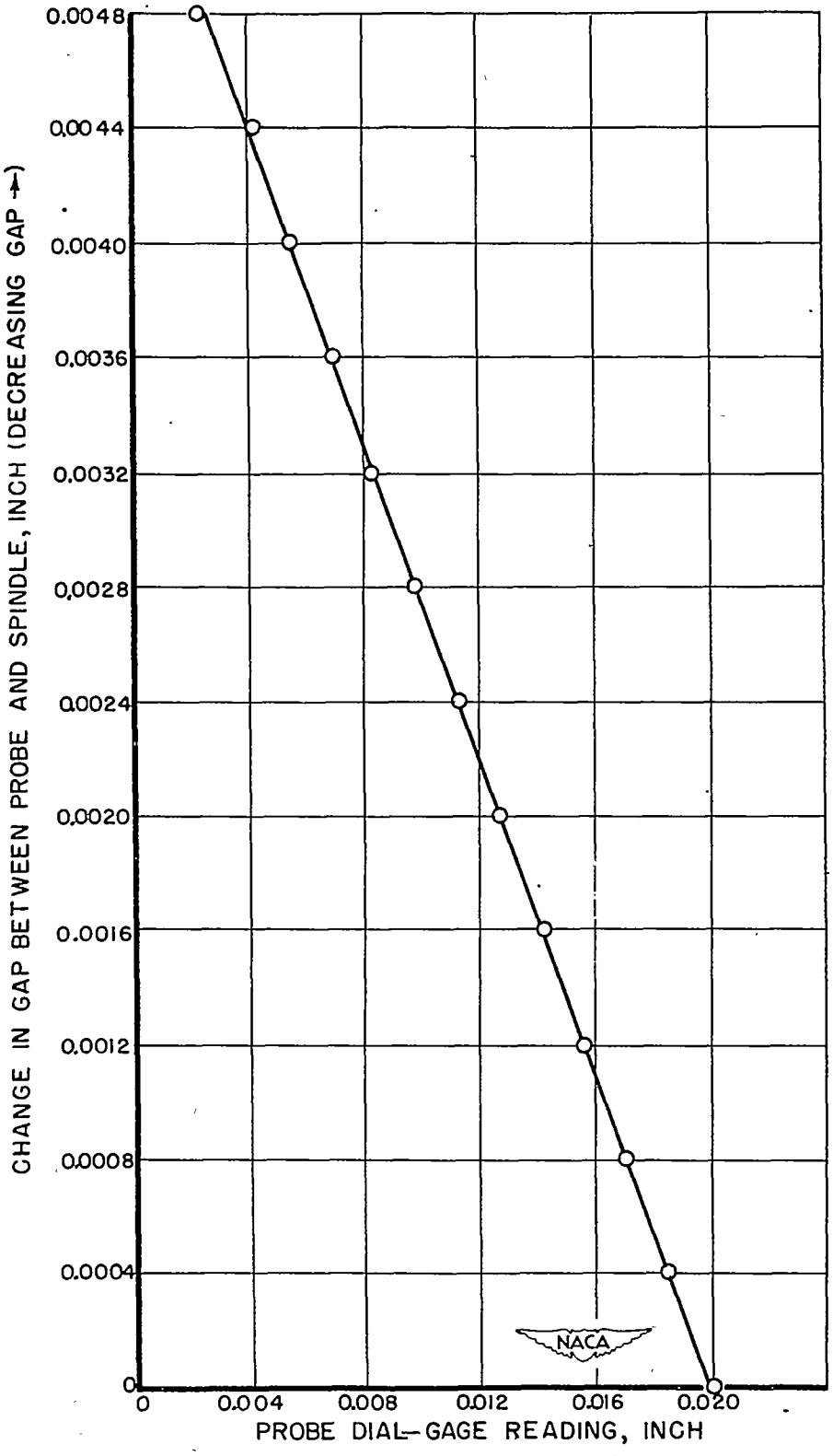

Figure 27.- Calibration curve for cantilevers of probe 1.

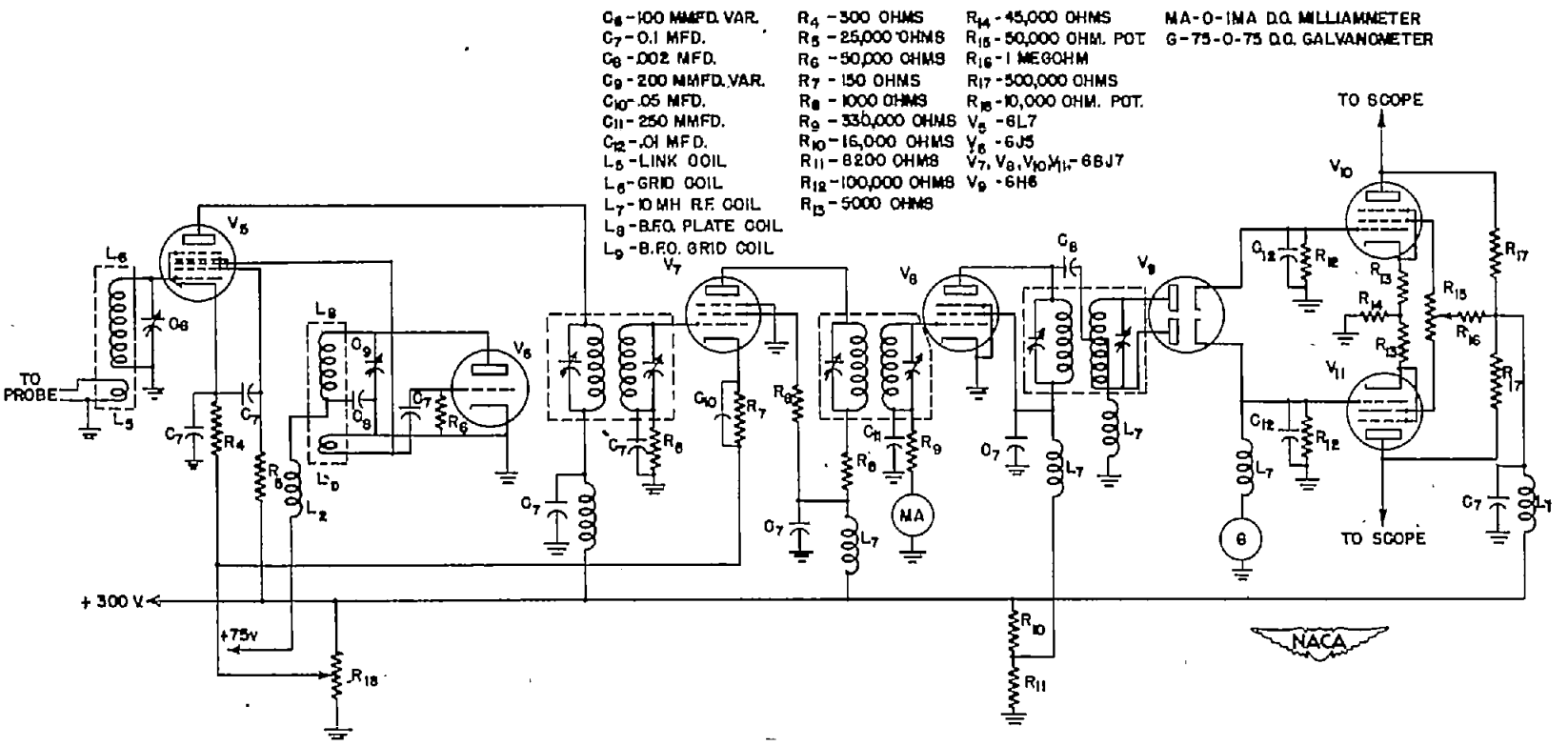

Figure 28.- Receiver circuit for frequency-modulation micrometer.

NACA-Langley - 11-15-51 - 1000

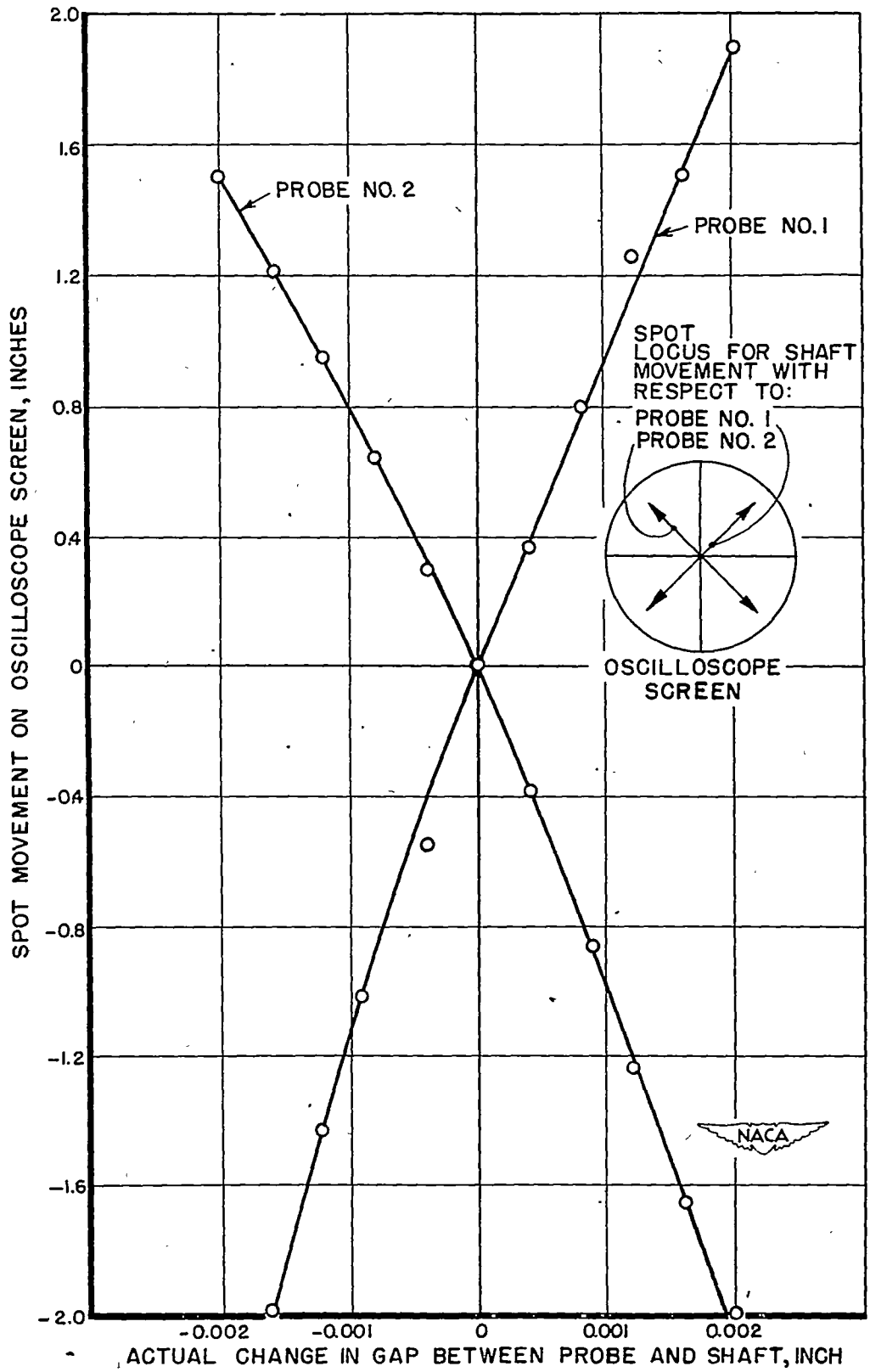

Figure 29.- Typical micrometer calibration curves.

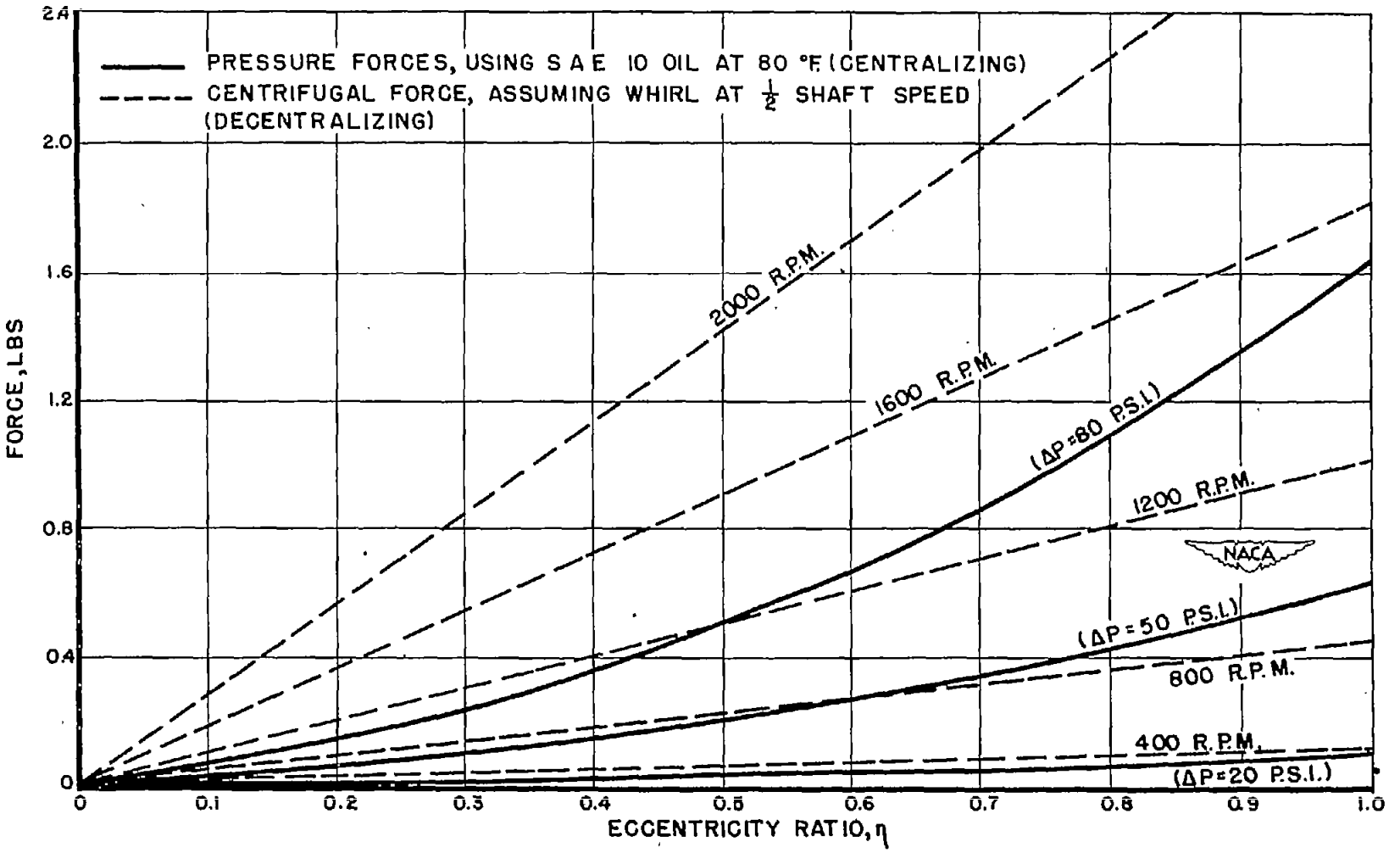

Figure 30.- Oil-pressure forces and centrifugal forces on a whirling journal.